



**HAL**  
open science

# Organotin(IV) trifluoromethanesulfonate chemistry: isolation and characterization of novel 1,10-phenanthroline-based derivatives

Hélène Cattey, Laurent Plasseraud

► **To cite this version:**

Hélène Cattey, Laurent Plasseraud. Organotin(IV) trifluoromethanesulfonate chemistry: isolation and characterization of novel 1,10-phenanthroline-based derivatives. *Comptes Rendus. Chimie*, 2024, 27 (S1), pp.1 - 18. 10.5802/crchim.260 . hal-04686844

**HAL Id: hal-04686844**

**<https://hal.science/hal-04686844v1>**

Submitted on 4 Sep 2024

**HAL** is a multi-disciplinary open access archive for the deposit and dissemination of scientific research documents, whether they are published or not. The documents may come from teaching and research institutions in France or abroad, or from public or private research centers.

L'archive ouverte pluridisciplinaire **HAL**, est destinée au dépôt et à la diffusion de documents scientifiques de niveau recherche, publiés ou non, émanant des établissements d'enseignement et de recherche français ou étrangers, des laboratoires publics ou privés.



ACADÉMIE  
DES SCIENCES  
INSTITUT DE FRANCE

# *Comptes Rendus*

---

## *Chimie*

Hélène Cattey and Laurent Plasseraud


**Organotin(IV) trifluoromethanesulfonate chemistry: isolation and characterization of novel 1,10-phenanthroline-based derivatives**

Published online: 13 May 2024

**Part of Special Issue:** French/Nordic Special Issue on Materials and Coordination Chemistry

**Guest editors:** Claude P. Gros (Université de Bourgogne, Dijon, France) and Abhik Ghosh (The Arctic University, UiT, Tromsø, Norway)

<https://doi.org/10.5802/crchim.260>

 This article is licensed under the  
CREATIVE COMMONS ATTRIBUTION 4.0 INTERNATIONAL LICENSE.  
<http://creativecommons.org/licenses/by/4.0/>



*The Comptes Rendus. Chimie are a member of the  
Mersenne Center for open scientific publishing*  
[www.centre-mersenne.org](http://www.centre-mersenne.org) — e-ISSN : 1878-1543



Research article

French/Nordic Special Issue on Materials and Coordination Chemistry

# Organotin(IV) trifluoromethanesulfonate chemistry: isolation and characterization of novel 1,10-phenanthroline-based derivatives

Hélène Cattey<sup>✉,a</sup> and Laurent Plasseraud<sup>✉,\*,a</sup>

<sup>a</sup> Institut de Chimie Moléculaire de l'Université de Bourgogne, UMR-CNRS 6302, Université de Bourgogne, 9 avenue A. Savary, F-21078 Dijon, France

E-mails: [helene.cattey@u-bourgogne.fr](mailto:helene.cattey@u-bourgogne.fr) (H. Cattey), [laurent.plasseraud@u-bourgogne.fr](mailto:laurent.plasseraud@u-bourgogne.fr) (L. Plasseraud)

**Abstract.** The reactivity of the hydroxo di-*n*-butyltin trifluoromethanesulfonato dimer complex [*n*-Bu<sub>2</sub>Sn(μ-OH)(H<sub>2</sub>O)(CF<sub>3</sub>SO<sub>3</sub>)<sub>2</sub>] (1) toward 1,10-phenanthroline (phen) has been investigated, leading to the formation of two novel di-*n*-butyltin(IV) trifluoromethanesulfonate complexes [*n*-Bu<sub>2</sub>Sn(μ-OH)(phen)]<sub>2</sub>[CF<sub>3</sub>SO<sub>3</sub>]<sub>2</sub> (5) and [*n*-Bu<sub>2</sub>Sn(phen)<sub>2</sub>][CF<sub>3</sub>SO<sub>3</sub>]<sub>2</sub> (6), in which the tin atoms are bis-chelated by one and two bidentate phen ligands, respectively. Salts 5 and 6 were characterized by single crystal X-ray diffraction analysis, elemental analysis, mass spectrometry, and infrared spectroscopy as well as <sup>1</sup>H, <sup>19</sup>F, <sup>13</sup>C{<sup>1</sup>H}, and <sup>119</sup>Sn{<sup>1</sup>H} NMR spectroscopy. Monitoring by <sup>119</sup>Sn{<sup>1</sup>H} NMR spectroscopy in CD<sub>3</sub>CN solution of the reaction proceeding with successive addition of phen revealed the *in situ* formation of three organotin(IV) trifluoromethanesulfonate intermediate species. Two of these, namely {[*n*-Bu<sub>2</sub>Sn(H<sub>2</sub>O)]<sub>2</sub>O·*n*-Bu<sub>2</sub>Sn(OH)<sub>2</sub>}[CF<sub>3</sub>SO<sub>3</sub>]<sub>2</sub> (2) and [*n*-Bu<sub>2</sub>Sn<sub>2</sub>(OH)(CF<sub>3</sub>SO<sub>3</sub>)<sub>2</sub>O] (4), were already known and could be clearly identified on the basis of their <sup>119</sup>Sn{<sup>119</sup>H} NMR chemical shifts. The composition of the third intermediate, 3, with an unknown chemical shift value, was investigated. A possible structure, especially suggested by electrospray-ionization mass spectrometry, is proposed as {[*n*-Bu<sub>2</sub>Sn(phen)(CF<sub>3</sub>SO<sub>3</sub>)<sub>2</sub>(μ-CF<sub>3</sub>SO<sub>3</sub>)]}[CF<sub>3</sub>SO<sub>3</sub>]. Furthermore, from a mixture of 1 and phen in equimolar ratio, in dichloromethane solvent and at -20 °C, temperature-sensitive crystals of a new hydrated di-*n*-butyltin cation, [*n*-Bu<sub>2</sub>Sn(phen)(OH)(H<sub>2</sub>O)]<sup>+</sup>[CF<sub>3</sub>SO<sub>3</sub>]<sup>-</sup> (7), were isolated. Crystals of the organic salt 1,10-phenanthroline trifluoromethanesulfonate (phenHOTf) were also obtained from the filtrate of the mother-liquor. The reactivity of 1 toward 2,9-dimethyl-1,10-phenanthroline was also explored (dmphen), leading to the detection of characteristic fingerprints of distannoxanes 2 and 4 by <sup>119</sup>Sn{<sup>119</sup>H} NMR, and to the crystallization of phenanthroline triflate salts, which were characterized by X-ray diffraction analysis as dmphenHOTf and dmphenHOTf·dmphen.

**Keywords.** Di-*n*-butyltin(IV) complexes, Trifluoromethanesulfonate anion, Nitrogen-containing heterocyclic compounds, 1,10-Phenanthroline derivatives, <sup>119</sup>Sn{<sup>1</sup>H} NMR monitoring, Single crystal X-ray diffraction.

Manuscript received 28 April 2023, revised 19 July 2023, accepted 4 September 2023.

\* Corresponding author.

## 1. Introduction

To the best of our knowledge, the first study describing the synthesis of organotin trifluoromethanesulfonates dates back to the 1970s, led by Schmeißer's group [1]. Since then, this class of compounds has attracted much interest in homogeneous catalysis and synthesis. These compounds are indeed reported to be efficient for specific metal-assisted organic reactions, acting as appropriate *Lewis* acid catalysts. Beneficial effects have been particularly described for the aldol reaction of *Mukaiyama* [2], *Robinson* annulation [3], acetylation of alcohols [4], transesterification of dimethyl carbonate with phenol [5], and direct synthesis of dimethyl carbonate (DMC) from methanol and carbon dioxide [6,7]. From a synthetic point of view, organotin trifluoromethanesulfonates are generally prepared by reacting an organotin oxide with trifluoromethanesulfonic acid ( $\text{CF}_3\text{SO}_3\text{H}$ , TfOH) [8,9], or alternatively, from an organotin chloride ( $\text{R}_{(4-x)}\text{SnCl}_x$  with  $\text{R} = \text{alkyl}$ ) in the presence of silver trifluoromethanesulfonate ( $\text{AgCF}_3\text{SO}_3$ ) [8,10]. Several organotin(IV) complexes have been characterized in the solid state by single crystal X-ray analysis. The  $\text{CF}_3\text{SO}_3$  group can be ionic and behave as a counter anion, or be a ligand directly bound to tin. In the latter case, it can adopt various coordination modes. Examples of mono-, bi-, and tridentate as well as terminal, *pseudo*-terminal, and bridging  $\text{CF}_3\text{SO}_3$  groups have already been reported in the literature for *p*-block metals and are shown in Scheme 1 [11,12].

The chemistry and structural aspects of organotin trifluoromethanesulfonates were first reviewed by Beckmann in 2005 [13]. Since 2006, our group has also contributed to this field by characterizing several new specimens by X-ray crystallographic analysis: (i) ionic monobenzyltin(IV) trifluoromethanesulfonate clusters exhibiting unprecedented  $\text{Sn}_6$ ,  $\text{Sn}_{11}$ , and  $\text{Sn}_{12}$  frameworks [14,15], (ii) a two-dimensional organostannoxane coordination network  $\infty\{[n\text{-Bu}_2(\mu\text{-OH})\text{SnOSn}(\mu\text{-}\eta^2\text{-O}_3\text{SCF}_3)n\text{-Bu}_2]_2[n\text{-Bu}_2(\eta^1\text{-O}_3\text{SCF}_3)\text{SnOSn}(\mu\text{-OH})n\text{-Bu}_2]_2\}$  [12], which was found to be a polymorph of the tetra-*n*-butyldistannoxane trifluoromethanesulfonate cluster,  $[n\text{-Bu}_2\text{Sn}_2(\text{OH})(\text{CF}_3\text{SO}_3)]_2\text{O}$  (**4**), described initially by Otera [16,17], (iii) a polymeric chain of dimeric hydroxo di-*n*-butyltin(IV) units bridged by trifluoromethanesulfonate ligands,  $[\text{Sn}_2(\text{CF}_3\text{O}_3\text{S})_2(\text{C}_4\text{H}_9)_4(\text{OH})_2]_n$  [10]. More

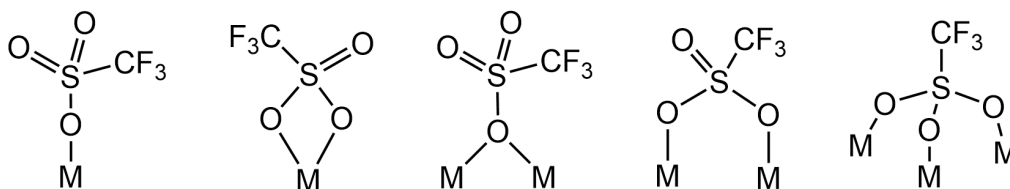
recently, we reported the isolation and characterization of the dihydrated di-*n*-butyltin(IV) trifluoromethanesulfonate salt  $\{[n\text{-Bu}_2\text{Sn}(\text{H}_2\text{O})]_2\text{O}\cdot n\text{-Bu}_2\text{Sn}(\text{OH})_2\}[\text{CF}_3\text{SO}_3]_2$  (**2**), which is characterized by a  $\text{Sn}_3\text{O}_3$  core [18]. **2** was obtained by reacting at room temperature with the dimeric hydroxo di-*n*-butyl trifluoromethanesulfonate  $[n\text{-Bu}_2\text{Sn}(\mu\text{-OH})(\text{H}_2\text{O})(\text{CF}_3\text{SO}_3)]_2$  (**1**) with a mixture of anthracene and phenazine.

Continuing to explore the reactivity of **1** toward nitrogen-containing heterocyclic compounds, we report herein the synthesis and characterization of two novel diorganotin trifluoromethanesulfonate derivatives,  $[n\text{-Bu}_2\text{Sn}(\mu\text{-OH})(\text{phen})]_2[\text{CF}_3\text{SO}_3]_2$  (**5**) and  $[n\text{-Bu}_2\text{Sn}(\text{phen})_2][\text{CF}_3\text{SO}_3]_2$  (**6**), resulting from the reaction of **1** with 1,10-phenanthroline (phen), with the latter acting as bidentate ligand. Monitoring of the reaction by  $^{119}\text{Sn}\{^1\text{H}\}$  NMR spectroscopy in solution ( $\text{CD}_3\text{CN}$ ) and as a function of the amount of phen added revealed successive *in situ* formation of species **2**, **3**, and **4**. From the three molar equivalents of phen, only the resonance of **5** is visible in the spectrum. Species **2** and **4** have already been reported in the literature; however, to the best of our knowledge, **3** is a new species. Complexes **5** and **6** were fully characterized by IR,  $^1\text{H}$ ,  $^{119}\text{F}$ ,  $^{13}\text{C}$ , and  $^{119}\text{Sn}\{^1\text{H}\}$  NMR spectroscopy, mass spectrometry, elemental analysis, and X-ray diffraction analysis. Further investigations were conducted to isolate and identify species **3**. By changing the solvent conditions from acetonitrile to dichloromethane and in a 1:1 molar ratio of **1** and phen, the unprecedented mononuclear hydrated di-*n*-butyltin cation,  $[n\text{-Bu}_2\text{Sn}(\text{phen})(\text{OH})(\text{H}_2\text{O})][\text{CF}_3\text{SO}_3]$  (**7**), was isolated, with the tin center *N,N*-chelated by a bidentate phen ligand and bearing a terminal hydroxyl group. Moreover, the reactivity of **1** was also tested in the presence of 2,9-dimethyl-1,10-phenanthroline (dmphen). From this reaction, only the phenanthrolium triflates (**dmphenHOTf** and **dmphen-dmphenHOTf**), resulting from the mono-protonation of dmphen, were obtained.

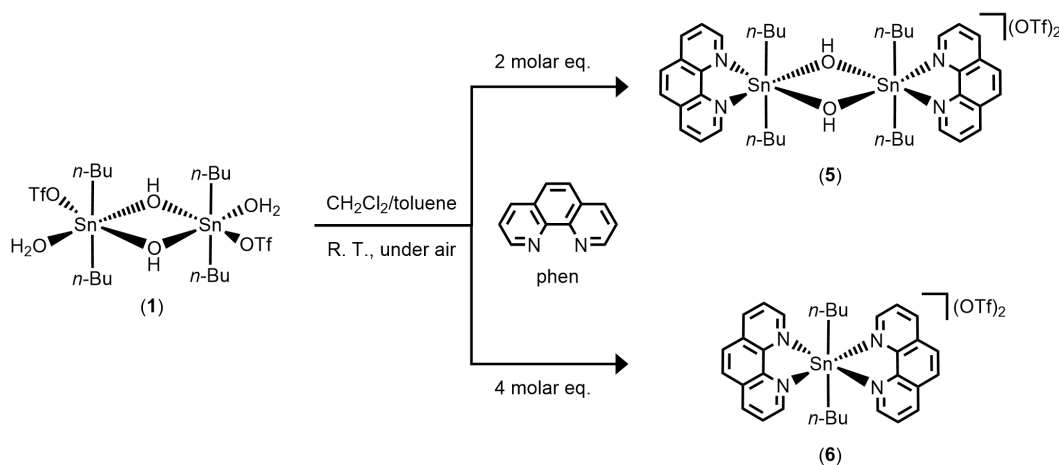
## 2. Results and discussion

### 2.1. Synthesis and isolation of $[n\text{-Bu}_2\text{Sn}(\mu\text{-OH})(\text{Phen})]_2[\text{CF}_3\text{SO}_3]_2$ (**5**) and $[n\text{-Bu}_2\text{Sn}(\text{Phen})_2][\text{CF}_3\text{SO}_3]_2$ (**6**)

The air-stable dinuclear di-*n*-butyltin(IV) trifluoromethanesulfonate salts  $[n\text{-Bu}_2\text{Sn}(\mu\text{-OH})(\text{phen})]_2$



**Scheme 1.** Molecular representations of known coordination modes involving the trifluoromethanesulfonate ligand and *p*-block metals (M).



**Scheme 2.** Synthetic pathway leading to 5 and 6.

$[\text{CF}_3\text{SO}_3]_2$  (5) and  $[\text{n-Bu}_2\text{Sn}(\text{phen})_2][\text{CF}_3\text{SO}_3]_2$  (6) were obtained at room temperature, under air atmosphere, from a mixture of dichloromethane/toluene by reacting dimeric trifluoromethanesulfonato hydroxo organotin(IV)  $[\text{n-Bu}_2\text{Sn}(\text{OH})(\text{H}_2\text{O})(\text{CF}_3\text{SO}_3)]_2$  (1) with two molar equivalents of 1,10-phenanthroline ( $\text{C}_{12}\text{H}_8\text{N}_2$ , phen) (Scheme 2). A pinkish precipitate is first formed, leading, after recrystallization in dichloromethane/toluene, to the formation of single crystals later characterized as 6. Colorless single crystals of 5 were obtained from the filtrate of the mother liquor by slow evaporation at room temperature.

The two new organotin compounds which are ionic were characterized by elemental analysis, ESI-MS, IR and NMR spectroscopy, and single-crystal X-ray diffraction analysis. Compound 5 exhibits good solubility in organic solvents such as dichloromethane, acetone, and acetonitrile. In  $\text{CD}_3\text{CN}$ , the  $^{119}\text{Sn}\{^1\text{H}\}$  NMR spectrum of 5 exhibits one single resonance at  $\delta -226$  ppm (Figure S1). Such a chemical shift is in agreement with a six-coordinate

tin atom substituted by two *n*-butyl moieties. It is interesting to note that in acetone- $d_6$ , the signal moves significantly, shifting to  $-150$  ppm, suggesting that the tin center is pentacoordinated in this solvent environment. For comparison, the tin atoms of  $[\text{n-Bu}_2\text{Sn}_2(\text{OH})(\text{CF}_3\text{SO}_3)]_2\text{O}$  (4), which is characterized as a distannoxane, exhibit two resonances in acetone- $d_6$  at  $-146$  and  $-151$  ppm [9,12]. The  $^1\text{H}$  and  $^{13}\text{C}\{^1\text{H}\}$  NMR spectra of 5 depicted in Figures S2 and S3, respectively, corroborate the structure depicted in Scheme 2, showing two sets of signals characteristic of phenanthroline ligands and *n*-butyl substituents. The  $\text{CF}_3$  moieties of the  $\text{CF}_3\text{SO}_3^-$  anions are also clearly identified in the  $^{13}\text{C}\{^1\text{H}\}$  NMR spectrum, giving a typical quartet at  $\delta 119.9$  ppm, with a distinctive  $^1J_{\text{C-F}}$  coupling constant of 318 Hz. The  $^{19}\text{F}$  NMR spectrum exhibits one singlet at  $\delta -78.2$  ppm (Figure S4). The infrared spectrum of 5 highlights a distinctive broad absorption centered at  $3321\text{ cm}^{-1}$  (Figure 1b), which is quite different from the fingerprint of 1 (Figure 1a), but can be assigned to the presence of OH groups (Figure 1b). Characteristic vibration bands of trifluoromethanesulfonate lig-

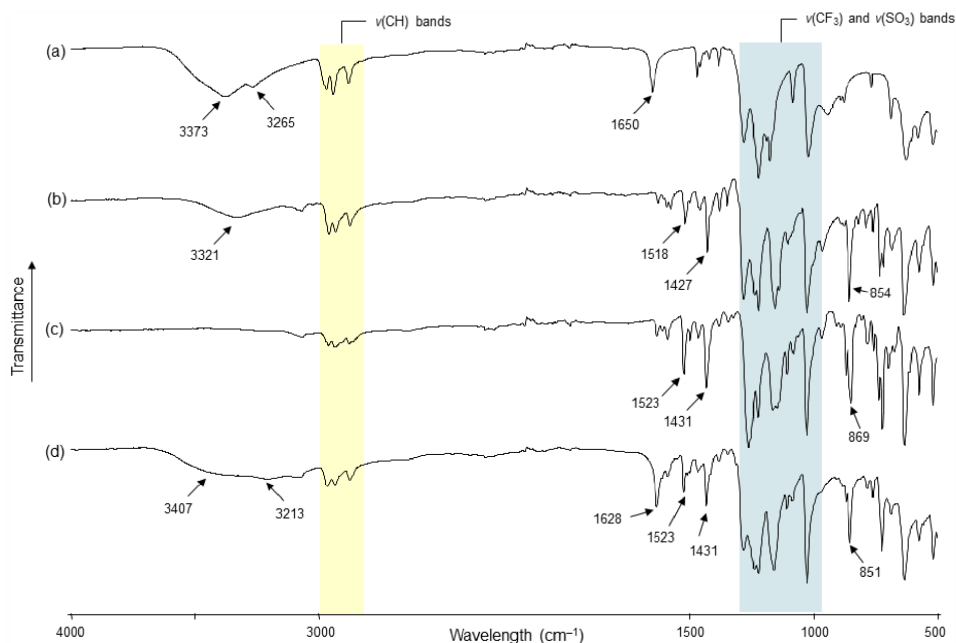


**Figure 1.** FT-IR (ATR) spectra of (a)  $[n\text{-Bu}_2\text{Sn}(\text{OH})(\text{H}_2\text{O})(\text{CF}_3\text{SO}_3)]_2$  (**1**), (b)  $[n\text{-Bu}_2\text{Sn}(\mu\text{-OH})(\text{phen})]_2[\text{CF}_3\text{SO}_3]_2$  (**5**), (c)  $[n\text{-Bu}_2\text{Sn}(\text{phen})_2][\text{CF}_3\text{SO}_3]_2$  (**6**), and (d)  $[n\text{-Bu}_2\text{Sn}(\text{phen})(\text{OH})(\text{H}_2\text{O})][\text{CF}_3\text{SO}_3]$  (**7**).

ands, in particular  $\nu(\text{CF}_3)$  and  $\nu(\text{SO}_3)$ , are also observed for **3** in the stretching region between 1000 and 1300  $\text{cm}^{-1}$  (outlined by a blue banner in Figure 1) [19–21]. The additional intense bands at 1518, 1427 and 854  $\text{cm}^{-1}$  arise from the  $\nu(\text{C}=\text{C})$ ,  $\nu(\text{C}=\text{N})$  and  $\gamma(\text{C}-\text{H}$  aromatic rings) absorptions of the phen ligands, respectively. The coordination of these ligands to tin is supported by the shift of the two bands at 1518  $\text{cm}^{-1}$ , and 1427  $\text{cm}^{-1}$  relative to the free ligand (1503  $\text{cm}^{-1}$  and 1420  $\text{cm}^{-1}$ ) [22,23]. An electrospray mass spectrum (positive mode) of **5** in a mixture of dichloromethane/methanol displays major mass clusters centered at  $m/z = 431.11333$  Da (100%), which fits closely with the  $[n\text{-Bu}_2\text{Sn}(\text{OH})(\text{phen})]^+$  fragment ( $\text{C}_{20}\text{H}_{27}\text{N}_2\text{OSn}$ , calc.: 431.11453 Da) (Figure S5). Finally, the micro-analytical (C, H, N, S) data also support the composition of **5** (see Section 4).

Compound **6** was collected as a precipitate from the starting reaction. However, it was found to be well soluble in acetone and dichloromethane. Suitable single-crystals for X-ray diffraction analysis were grown from a dichloromethane/toluene mixture. Compared with **1** and **5**, the infrared spectrum of **6** shows no absorption bands above 3100  $\text{cm}^{-1}$  ex-

cluding the presence of OH or  $\text{H}_2\text{O}$  ligands. Otherwise, the characteristic absorption bands of  $n$ -butyl chain [ $\nu(\text{C}-\text{H})$ ],  $\text{CF}_3\text{SO}_3$ , and phen are present and support the coordination of the phen ligand to the tin center (Figure 1c). In the acetone- $d_6$  solution, the  $^{119}\text{Sn}\{^1\text{H}\}$  NMR of **6** reveals a broad resonance at  $\delta -231$  ppm (Figure S6) [for comparison, in the same deuterated solvent, **5** exhibits a weak resonance at  $\delta -150$  ppm (Figure S7)], and the  $^1\text{H}$  NMR spectrum shows a 1:1 integration ratio between the protons of the  $n$ -butyl chains and the phen ligands (Figure S8). The  $^{13}\text{C}\{^1\text{H}\}$  NMR spectrum exclusively reveals phen and  $n$ -butyl resonances and highlights the presence of  $\text{CF}_3\text{SO}_3^-$  anions by giving a quartet centered at  $\delta 121.9$  ppm, which is attributable to  $\text{CF}_3$  moieties ( $^1J_{\text{C}-\text{F}} = 321$  Hz) (Figure S9). A single resonance at  $\delta -78.8$  ppm is also observed in the  $^{19}\text{F}$  NMR spectrum (Figure S10). The electrospray mass spectrum (positive mode) of **6** in a mixture of dichloromethane/methanol displays two predominant mass clusters centred at  $m/z = 445.13055$  Da (100%) and 431.11559 Da (80%), which can be assigned to  $[n\text{-Bu}_2\text{Sn}(\text{phen})(\text{OCH}_3)]^+$  ( $\text{C}_{21}\text{H}_{29}\text{N}_2\text{OSn}$ , calc.: 445.13019 Da) and  $[n\text{-Bu}_2\text{Sn}(\text{phen})(\text{OH})]^+$  ( $\text{C}_{20}\text{H}_{27}\text{N}_2\text{OSn}$ , calc.: 431.11454 Da) fragments, respectively (Figure S11).

## 2.2. Single-crystal X-ray diffraction analysis of **5**

The solid-state structure of **5** consists of a  $[n\text{-Bu}_2\text{Sn}(\text{OH})(\text{phen})]_2^{2+}$  dication surrounded by two non-coordinated  $\text{CF}_3\text{SO}_3^-$  anions. An ORTEP view of **5** is shown in Figure 2 together with the selected bond distances and angles. The inorganic core of the cation is based on a planar four-membered distannoxane  $[\text{Sn}_2(\mu\text{-OH})_2]$  unit, where the tin atoms are bridged by two hydroxide ligands. The two tin atoms are bound to two *n*-butyl ligands  $[\text{Sn}-\text{C}13 = 2.131(2)$ ,  $\text{Sn}-\text{C}17 = 2.128(2)$  Å], to two oxygen atoms of bridging hydroxide ligands  $[\text{Sn}-\text{O}1 = 2.0828(13)$ ,  $\text{Sn}-\text{O}1^i = 2.2334(14)$  Å], and are chelated by a bidentate 1,10-phenanthroline molecule forming five-membered rings. However, the Sn–N distances show significant differences  $[\text{Sn}-\text{N}1 = 2.4171(17)$ ,  $\text{Sn}-\text{N}2 = 2.6330(18)$  Å]. Thus, the tin centers can be considered to be hexacoordinated, adopting a markedly distorted octahedral geometry  $[\text{C}17-\text{Sn}-\text{C}13 = 156.93(9)^\circ$ ,  $\text{N}1-\text{Sn}-\text{O}1^i = 156.85(5)^\circ$ ,  $\text{N}2-\text{Sn}-\text{O}1 = 150.33(6)^\circ$ ]. Furthermore, the phen ligands are parallel to each other and exhibit a twist angle of  $25.55(4)^\circ$  to the plane containing the  $\text{Sn}_2\text{O}_2$  ring. Two trifluoromethanesulfonate anions complete the structure of **5**. For both  $\text{CF}_3\text{SO}_3^-$ , one of their oxygen atoms is involved in hydrogen interaction with a hydroxide group of the cation  $[\text{O}_3 \cdots \text{HO} = 2.791(2)$  Å]. Moreover, we can also suspect for each  $\text{CF}_3\text{SO}_3^-$  a possible weak interaction involving another oxygen atom of sulfonate functions and one tin atom of the cation  $[\text{O}4 \cdots \text{Sn} = 3.342(2)$  Å], which could explain the different Sn–N distances. The existence of such long-distance  $\text{Sn} \cdots \text{O}$  interactions in the solid state has already been underlined for previous diorganotin compounds [10,24]. In the past, *Blaschette* and *Jones* reported the isolation of  $[\text{Me}_2\{(\text{MeSO}_2)_2\text{N}\}(\text{phen})\text{Sn}(\mu\text{-OH})]_2$ , a compound structurally analogous to **5** and prepared from  $\text{Me}_2\text{Sn}[\text{N}(\text{SO}_2\text{Me})_2]_2$  and 1,10-phenanthroline by adventitious hydrolysis [25]. Interestingly, in this compound, the  $(\text{MeSO}_2)_2\text{N}^-$  anions operate in the same manner as the triflate anions of **5**. They are non-coordinated and are involved in hydrogen bonding and long  $\text{Sn} \cdots \text{O}$  interactions. The authors then described the tin atoms as being heptacoordinated in a pentagonal bipyramidal arrangement. With regard to compound **5** and based on the  $^{119}\text{Sn}\{^1\text{H}\}$  NMR chemical shift value ( $\delta = -226$  ppm in  $\text{CD}_3\text{CN}$ ), we

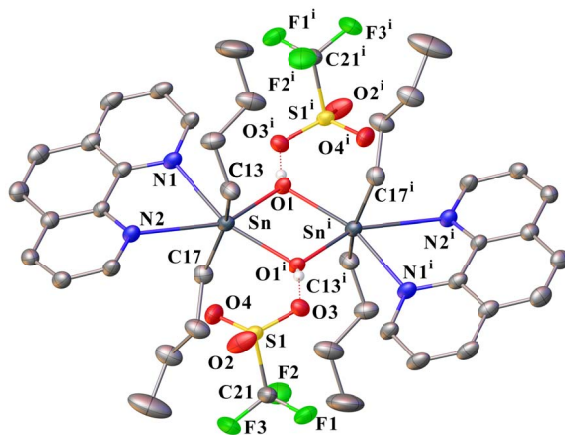


**Figure 2.** ORTEP drawing of **5** using a partial atom labeling scheme (30% probability thermal ellipsoids). Hydrogen atoms of phenanthroline ligands and *n*-butyl chains are omitted for clarity. Hydrogen bonds involving  $\text{CF}_3\text{SO}_3^-$  and  $\mu\text{-OH}$  groups are represented by red dotted lines. Selected bond lengths (Å) and angles ( $^\circ$ ): Sn–C17 2.128(2), Sn–C13 2.131(2), Sn–O1 2.0820(13), Sn–O1<sup>*i*</sup> 2.2343(14), Sn–N1 2.4171(17), C21–F3 1.315(3), C21–F1 1.329(3), C21–F2 1.334(3), C21–S1 1.816(3), S1–O2 1.4239(19), S1–O4 1.4331(18), S1–O3 1.4406(15); O1–Sn–C17 100.02(7), O1–Sn–C13 102.51(8), C17–Sn–C13 156.93(9), O1–Sn–O1<sup>*i*</sup> 72.08(6), C17–Sn–O1<sup>*i*</sup> 90.38(8), C13–Sn–O1<sup>*i*</sup> 91.85(8), O1–Sn–N1 84.98(6), C17–Sn–N1 90.58(8), C13–Sn–N1 96.24(8), O1<sup>*i*</sup>–Sn–N1 156.85(5), Sn–O1–Sn<sup>*i*</sup> 107.92(6), F3–C21–F1 107.0(2), F3–C21–F2 108.8(3), F1–C21–F2 106.7(2), F3–C21–S1 112.27(19), F1–C21–S1 110.9(2), F2–C21–S1 110.95(18), O2–S1–O4 116.03(13), O2–S1–O3 114.98(13), O4–S1–O3 113.25(10), O2–S1–C21 103.25(13), O4–S1–C21 104.76(13), O3–S1–C21 102.36(10) (symmetry transformations used to generate equivalent atoms: (<sup>*i*</sup>):  $3/2-x, 1/2-y, -z$ ).

argue in this case for the hexacoordination of the tin atoms.

## 2.3. Single-crystal X-ray structural analysis of **6**

The structure of salt **6** in the solid state consists of a  $[n\text{-Bu}_2\text{Sn}(\text{Phen})_2]^{2+}$  dication surrounded by

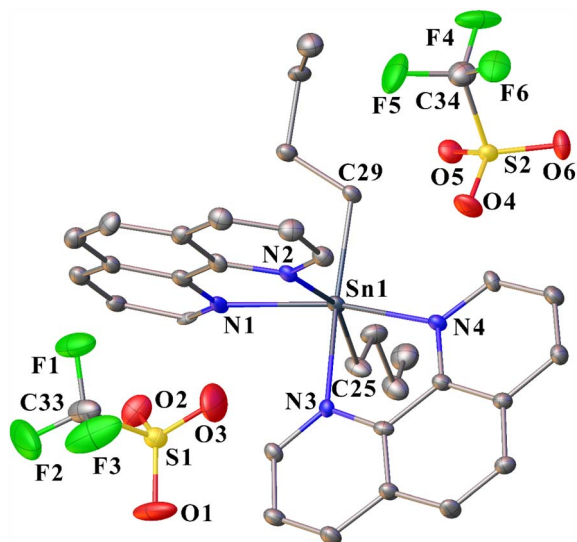


**Figure 3.** ORTEP drawing of **6** using a partial atom labeling scheme (30% probability thermal ellipsoids). Hydrogen atoms and one molecule of toluene (solvent) are omitted for clarity. Selected bond lengths (Å) and angles (°): Sn1–C29 2.162(9), Sn1–C25 2.158(9), Sn–N1 2.273(8), Sn–N2 2.369(8), Sn–N3 2.309(7), Sn–N4 2.275(8), S1–O2 1.415(8), S1–O1 1.427(8), S1–O3 1.431(9), S1–C33 1.823(11), C33–F1 1.299(12), C33–F2 1.328(14), C33–F3 1.312(13), C25–Sn1–C29 116.9(4), N1–Sn1–N2 71.9(3), N1–Sn1–N3 87.7(3), N1–Sn1–N4 154.5(3), C29–Sn1–N1 98.0(3), C25–Sn1–N1 97.0(4), N3–Sn1–N2 76.3(3), N4–Sn1–N2 87.5(3), C29–Sn1–N2 84.12(3), C25–Sn1–N2 157.9(3), N4–Sn1–N3 72.6(3), C29–Sn1–N3 156.9(3), C25–Sn1–N3 84.3(3), C29–Sn1–N4 94.6(3), C25–Sn1–N4 96.9(4).

two non-coordinating  $\text{CF}_3\text{SO}_3^-$  anions. One toluene molecule (crystallization solvent) co-crystallizes with **6**. Figure 3 shows an ORTEP view of **6** with the atom numbering scheme, and Figure 4 shows a perspective view of the crystal packing in the unit cell. The molecular structure of the title compound consists of a central six-coordinated tin atom that exhibits an octahedral coordination environment comprising four nitrogen atoms from two distinct chelating phen ligands and two carbon atoms of the two *n*-butyl chains. The ligands are positioned in a *cis*-arrangement. The N1–Sn–N4, N2–Sn–C25,

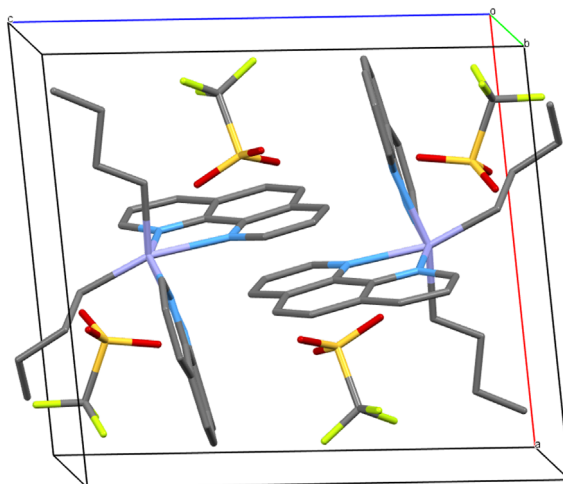


**Figure 4.** Projection of the crystal structure approximately along the *b* axis, showing the orientation of the phen ligands between two neighboring cations of **6**. The solvent toluene molecules co-crystallizing with **6** and hydrogen protons are omitted (MERCURY representation [27], color code: Sn = violet, N = blue, C = gray, O = red, S = yellow, F = green).

N3–Sn–C29 bond angles measure 154.5(3), 157.9(3), and 156.9(3)°, respectively, indicating a distortion from an ideal octahedral geometry. The two phen ligands are bidentate to tin, forming five-membered chelate rings that are nearly planar. The Sn–N distances are in the range of 2.273(8) and 2.368 Å. They are comparable to that found in  $[\text{MeSn}(\text{phen})_2]^{2+}$  [26], which is, to the best of our knowledge, the only example reported to date for a diorganotin complex bis-*N,N*-chelated by two 1,10-phenanthroline ligands.

From a supramolecular point of view, the molecules of **6** are organized in pairs *via* offset  $\pi$ – $\pi$  interactions involving the aromatic rings of each phen ligand (Figure 4). The interplanar and centroid-to-centroid distances between the two parallel phen molecules are 3.393 and 4.732 Å, respectively. In general, for such interactions, the interplanar distance is assumed to be in the range of 3.3–3.8 Å [28]. In the arrangement of **6**, the rings are severely offset with a slippage angle (angle between the normal to the planes and the centroid vector centroid vector) of 44.19°, which corresponds to a slip distance of 3.298 Å.



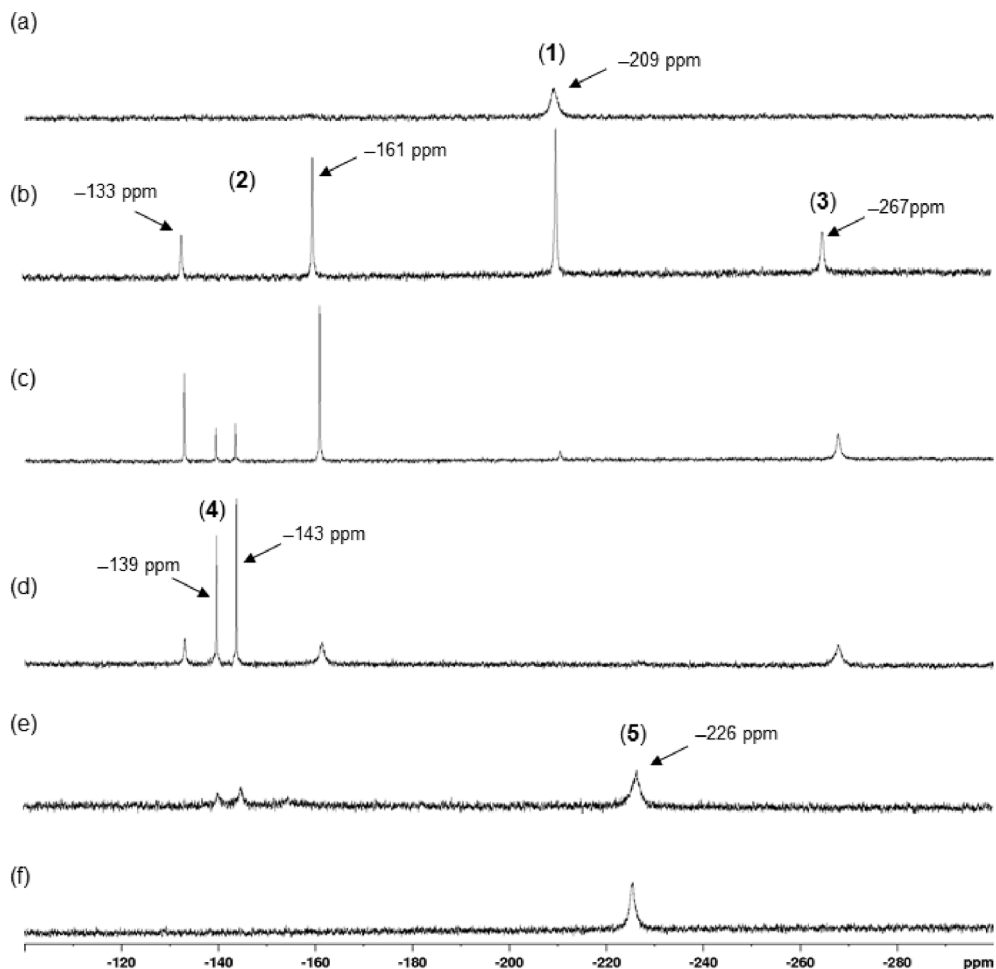
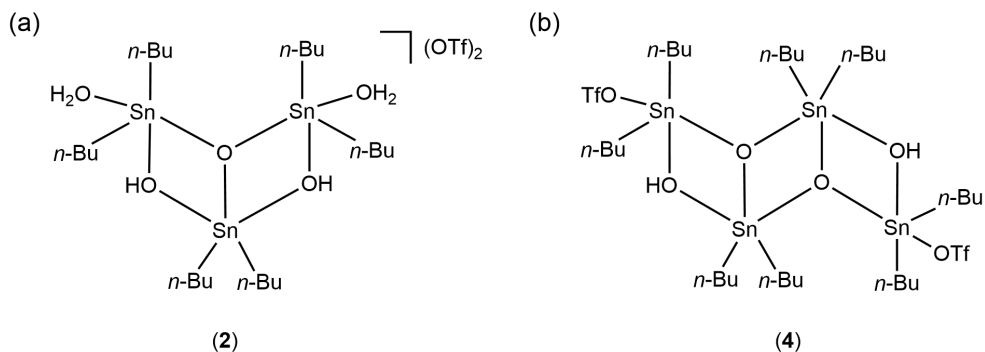


**Figure 5.**  $^{119}\text{Sn}\{^1\text{H}\}$  NMR monitoring of the evolution of a solution of **1** in  $\text{CD}_3\text{CN}$  ([0.08 M], 298 K) as a function of successive additions of 1,10-phenanthroline (phen): (a) starting solution of **1**, (b) after addition of 0.5 molar equivalent, (c) of 0.75 molar equivalent, (d) of 1 molar equivalent, (e) of 2 molar equivalent, and (f) of 3 molar equivalent.

#### 2.4. Solution $^{119}\text{Sn}\{^1\text{H}\}$ NMR monitoring

The reactivity of **1** toward successive additions of 1,10-phenanthroline was followed by  $^{119}\text{Sn}\{^1\text{H}\}$  spectroscopy in  $\text{CD}_3\text{CN}$  directly in an NMR tube, as shown in Figure 5. In  $\text{CD}_3\text{CN}$ , compound **1** shows a broad signal at  $\delta -209$  ppm in agreement with the value reported previously in the literature [8] (Figure 5a). The addition of 0.5 molar equivalents of phen leads to the appearance of three new signals at  $\delta -133$ ,  $-161$ , and  $-267$  ppm in addition to the signal of **1**, which is still present at  $\delta -209$  ppm (Figure 5b).

The two de-shielded chemical shifts exhibiting a 1:2 intensity ratio correspond to the signature of the ionic complex **2**, already known and characterized by us as the unusual trinuclear complex  $\{[n\text{-Bu}_2\text{Sn}(\text{H}_2\text{O})]_2\text{O}\cdot n\text{-Bu}_2\text{Sn}(\text{OH})_2\} [\text{CF}_3\text{SO}_3]_2$  (**2**) (Scheme 3a) [16], while the signal at  $\delta -267$  ppm can be attributed to a new species **3** whose composition and structure will be discussed later. Further addition of phen (up to 1 molar equivalent) lead to a progressive disappearance of the previously described resonances in favor of the emergence, and then the predominance, of a new pair of signals located at



**Scheme 3.** Molecular representations of **2** (a) and **4** (b).

**Table 1.**  $^{119}\text{Sn}\{^1\text{H}\}$  NMR chemical shift data of di-*n*-butyltin(IV) trifluoromethanesulfonates

Compounds	$\delta$ (ppm) <sup>a</sup>		
	In $\text{CD}_2\text{Cl}_2$	In acetone- <i>d</i> <sub>6</sub>	in $\text{CD}_3\text{CN}$
<b>1</b>	−145		−209
<b>2</b>	−127, −149 [18]		−133, −161
<b>3</b>	−288		−267
<b>4</b>	−135, −144 [18]	−146, −151 [12]	−139, −143
<b>5</b>	Not visible	−150	−226
<b>6</b>	Not visible	−231	Insoluble
<b>7</b>			−260

<sup>a</sup> At  $T = 298$  K.

−139 and −143 ppm (Figure 5b and c). They reflect the formation of 3-hydroxy-1-(triflate)tetra-*n*-butyldistannoxane,  $[\text{n-Bu}_2\text{Sn}_2(\text{OH})(\text{CF}_3\text{SO}_3)]_2\text{O}$  (**4**), whose solid-state structure was initially established by Otera *et al.* (Scheme 3b) [9]. For our part, we had previously shown the possible transformation of **2** to **4** in the presence of phenazine [16]. It is likely that a similar reaction can occur in the presence of 1,10-phenanthroline. When the addition of phen reaches two molar equivalents, the residual signals of **4** are still visible, but a broad resonance, prevailing, appears at  $\delta -226$  ppm (Figure 5e). This corresponds to the formation of complex **5**. In the presence of three molar equivalents, this compound is the only species detected in solution (Figure 5f). However, a white precipitate is also observed at the bottom of the NMR tube, which corresponds to complex **6** insoluble in  $\text{CD}_3\text{CN}$ . The values of the  $^{119}\text{Sn}\{^1\text{H}\}$  NMR chemical shifts of the different organotin species implicated in this study are summarized in Table 1.

### 2.5. Isolation and characterization of species **3**

During the monitoring of the reaction by  $^{119}\text{Sn}\{^1\text{H}\}$  NMR, all signals were attributed to identified organotin species, except for the single broad resonance at  $\delta -267$  ppm in  $\text{CD}_3\text{CN}$  (Figure S12), which was assigned to compound **3**. We did not find any bibliographic data associated with this species; therefore, it appeared to be new and its composition remains to be clarified. We first sought to isolate it by reproducing the experimental conditions of the NMR measurement depicted in Figure 5d in glassware conditions, i.e., by adding 1 molar equivalent of phen to a solution of **1** in a mixture of acetonitrile/toluene (15 mL/10 mL). After three successive separations by crystallization at 4 °C (**2** and **4** were collected as crystalline products) in a  $\text{CH}_3\text{CN}$ /toluene mixture, it was possible to isolate only **3**. After complete evaporation of the solvents, **3** consists of a colorless pasty solid. Infrared analysis, shown in Figure S13,

reveals several characteristic bands: (i)  $\nu(\text{C-H})$  absorption bands between 2800 and 3000  $\text{cm}^{-1}$ , (ii)  $\nu(\text{C=C})$ ,  $\nu(\text{C=N})$  and  $\delta(\text{C-H})$  fingerprints of the phen ligand [22,23], and (iii) stretching vibration bands of trifluoromethanesulfonate ligands [ $\nu(\text{CF}_3)$  and  $\nu(\text{SO}_3)$ ] between 1000 and 1300  $\text{cm}^{-1}$  [19–21]. A  $^{119}\text{Sn}\{^1\text{H}\}$  NMR spectrum of a solution of **3** in  $\text{CD}_2\text{Cl}_2$  shows a singlet resonance at  $\delta -288$  ppm. The  $^{13}\text{C}\{^1\text{H}\}$  NMR spectrum of **3** in  $\text{CD}_2\text{Cl}_2$  (Figure S14) highlights two sets of signals attributed to the presence of *n*-butyl and phenanthroline ligands. A quartet at  $\delta$  121.2 ppm ( $^1J_{\text{C-F}} = 320$  Hz) reveals the presence of  $\text{CF}_3$  moieties, which is corroborated by the  $^{19}\text{F}$  NMR spectrum, which exhibits one singlet at  $\delta -78.4$  ppm (Figure S15). The  $^1\text{H}$  spectrum establishes a phen/*n*-butyl ligand ratio of 1:2 (Figure S16). The electrospray mass spectrum (positive mode) of **3** in dichloromethane/acetonitrile solution displays three intense mass clusters (Figure S17). The first one centered at  $m/z = 563.0613$  Da ( $z = 1$ , 67%) matches with high accuracy to a mononuclear di-*n*-butyltin fragment bearing a positive charge that can be assigned to  $[\text{n-Bu}_2\text{Sn}(\text{phen})(\text{CF}_3\text{SO}_3)]^+$  ( $\text{C}_{21}\text{H}_{26}\text{O}_3\text{N}_2\text{F}_3\text{SSn}$ , calc. = 563.0628 Da), whereas the cluster centered at  $m/z = 1275.07507$  Da ( $z = 1$ , 100%) is consistent with the monocationic dinuclear framework of the empirical formula  $\text{C}_{43}\text{H}_{52}\text{O}_9\text{N}_4\text{F}_9\text{S}_3\text{Sn}_2$  (calc. = 1275.07912 Da). The intermediate cluster at  $m/z = 893.0887$  Da (67%) is compatible with  $[\text{M}+\text{H-phen-n-Bu}_2\text{Sn}]^+$  ( $\text{C}_{34}\text{H}_{35}\text{O}_6\text{N}_4\text{F}_6\text{S}_2\text{Sn}$ , calc. = 893.0819 Da). Simulations of these ESI-MS mass clusters are depicted in Figures S18–S20. On the basis of these data, we suggest that for species **3**, the structure reproduced on Figure 6 could correspond to two  $[\text{n-Bu}_2\text{Sn}(\text{phen})(\text{CF}_3\text{SO}_3)]$  entities bounded by a bridging trifluoromethanesulfonate ligand,  $[\{\text{n-Bu}_2\text{Sn}(\text{phen})(\text{CF}_3\text{SO}_3)\}_2(\mu\text{-CF}_3\text{SO}_3)][\text{CF}_3\text{SO}_3]$ . The overall positive charge of **3** is compensated by an  $\text{CF}_3\text{SO}_3^-$  anion. To the best of our knowledge, such a structure has not yet been described in the literature. However, there are some reports confirming in the solid-state the existence of  $-\text{CF}_3\text{SO}_3$  groups bridging di-*n*-butyltin derivatives. In general, this results in the propagation of polymeric networks:  $[\text{Sn}_2(\text{CF}_3\text{O}_3\text{S})_2(\text{C}_4\text{H}_9)_4(\text{OH})_2]_n$  [10],  ${}_{\infty}^2\{[\text{n-Bu}_2(\mu\text{-OH})\text{SnOSn}(\mu\text{-}\eta^2\text{-OSO}_2\text{CF}_3)\text{n-Bu}_2]\}$  [9],  ${}_{\infty}^2\{[\text{n-Bu}_2(\mu\text{-OH})\text{SnOSn}(\mu\text{-}\eta^2\text{-O}_3\text{SCF}_3)\text{n-Bu}_2]_2[\text{n-Bu}_2(\eta^1\text{-O}_3\text{SCF}_3)\text{SnOSn}(\mu\text{-OH})\text{n-Bu}_2]_2\}$  [12]. In

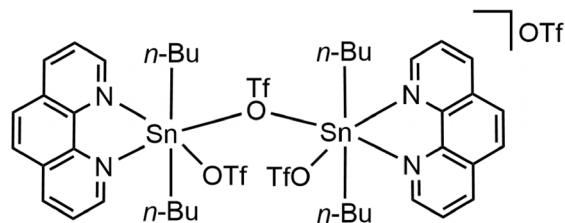


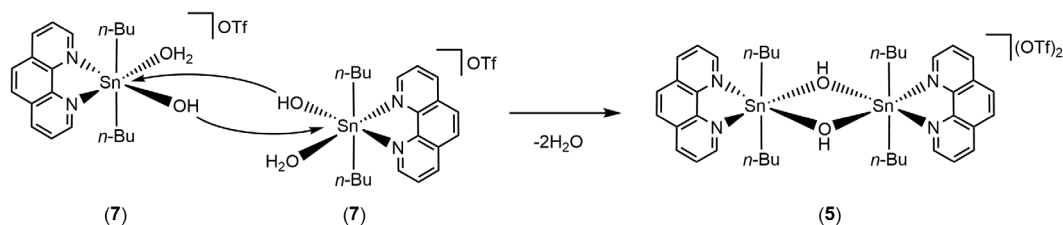
**Figure 6.** Possible molecular representation of **3** (OTf =  $\text{CF}_3\text{SO}_3$ ).

**3**, the presence of phen ligands occupying two coordination sites on each tin atom probably prevents polymerization. In the context of the related chemistry of organotin(IV) alkanesulphonates, Shankar *et al.* recently reported the solid-state structures of di-*n*-butyltin complexes with bridging and terminal  $-\text{OSO}_2\text{R}$  ligands (R = Me, Et), quite comparable to the structure suspected for **3** [29].

The elemental analysis calculated for  $[\{\text{n-Bu}_2\text{Sn}(\text{phen})(\text{CF}_3\text{SO}_3)\}_2(\mu\text{-CF}_3\text{SO}_3)][\text{CF}_3\text{SO}_3]$  ( $\text{C}_{44}\text{H}_{52}\text{F}_{12}\text{N}_4\text{O}_{12}\text{S}_4\text{Sn}_2$ , 1422.57  $\text{g}\cdot\text{mol}^{-1}$ ) is also in accordance with the formula suggested for **3**: Calculated: C, 37.17; H, 3.68; N, 3.94; S, 9.02 Found: C, 36.43; H, 3.74; N, 4.13; S, 8.16%. Furthermore, as highlighted by the NMR measurements reported in Figures 5d and 5e, we verified that the addition of phen to a solution of **3** in CDCN does indeed result in the appearance of the characteristic signal of **5** at  $\delta -227$  ppm. However, to date, it was not possible to confirm the proposed structure by single crystal X-ray diffraction analysis because the compound does not crystallize properly in acetonitrile.

## 2.6. Reactivity in dichloromethane

In contrast, when the reaction between **1** and phen (in 1:1 molar ratio) is conducted in dichloromethane instead of acetonitrile, colourless single crystals are grown at  $-20$  °C from the filtrate of the reaction. They are unstable and melt very quickly as the temperature increases. This is recurrent and was observed in several batches. The crystallographic analysis could be performed despite the poor quality of crystals. However, several difficulties were encountered during the treatment of the crystallographic data: (i) the determination of the space group was delicate and

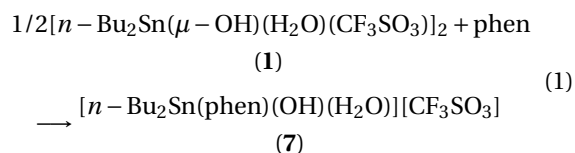


**Scheme 4.** Plausible mechanism leading to the formation of **5** from **7**.

finally defined as C2/c, (ii) several ligands were affected by disorders, (iii) a solvent-accessible voids remained. The resolution of the structure remains imperfect, but we believe that the structural data provided are informative in relation to the intermediate species leading to **5** and **6**. Thus, the structure of compound **7** (Figure 7) established the presence of a cationic mononuclear compound based on a tin atom carrying two *n*-butyl chains [Sn–C13 = 2.136(7), Sn–C17 = 2.123(7) Å] in *trans*-position with respect to each other and chelated by a bidentate phenanthroline ligand [Sn–N1 = 2.208(11), Sn–N2 = 2.342(8) Å]. The Sn–N bond lengths are comparable with those measured for **6**. Two oxygen atoms, O1 and O2, complete the coordination sphere of the tin atom, which describes a distorted octahedral geometry [N1–Sn–O1 = 157.1(3), N2–Sn–O2 = 162.2(3), C17–Sn–C13 = 156.89(9)]. The O1 and O2 atoms are assigned to OH<sub>2</sub> and OH ligands, respectively, but unfortunately, their hydrogen atoms could not be located. Their assignments were nevertheless possible based on the Sn–O interatomic distances, which are significantly different: Sn1–O1 = 2.512(8), as opposed to Sn–O2 = 2.142(5) Å. Distances greater than 2.3 Å have already been observed for several di-*n*-butyltin derivatives with Sn–OH<sub>2</sub> bonds: 2.365 Å in [*n*-Bu<sub>2</sub>Sn(H<sub>2</sub>O)(μ-OH)]<sub>2</sub>[CF<sub>3</sub>SO<sub>3</sub>] [5], 2.409 Å in [*n*-Bu<sub>2</sub>Sn(μ-OH)(H<sub>2</sub>O)(CF<sub>3</sub>SO<sub>3</sub>)]<sub>2</sub> [4], 2.511 Å in {[*n*-Bu<sub>2</sub>Sn(H<sub>2</sub>O)]<sub>2</sub>O·*n*-Bu<sub>2</sub>Sn(OH)<sub>2</sub>}[CF<sub>3</sub>SO<sub>3</sub>]<sub>2</sub> [16]. Sn–OH bonds are generally shorter: between 2.062 and 2.150 Å in [*n*-Bu<sub>2</sub>Sn(H<sub>2</sub>O)(μ-OH)]<sub>2</sub>[CF<sub>3</sub>SO<sub>3</sub>] [5], 2.120 Å in {[*n*-Bu<sub>2</sub>Sn(H<sub>2</sub>O)]<sub>2</sub>O·*n*-Bu<sub>2</sub>Sn(OH)<sub>2</sub>}[CF<sub>3</sub>SO<sub>3</sub>]<sub>2</sub> [16]. These examples support the attribution of O1 and O2. The positive charge of [*n*-Bu<sub>2</sub>Sn(phen)(OH)(H<sub>2</sub>O)]<sup>+</sup> is compensated by one non-coordinated CF<sub>3</sub>SO<sub>3</sub><sup>−</sup> anion. To the best of our knowledge, such a structure describing a monomeric complex is unprecedented. Diorganotin hydroxides are difficult to purify and character-

ize [30]. In the solid state, they are mainly described as dimers, hydroxyl groups acting as bridging ligands between two tin atoms, and also as polymers. Thus, the number of complexes with an OH group singly coordinated to tin is very limited [31–33]. In the case of **7**, although the resolution of its structure is not optimal, we assume that the coordination of the phen ligand favours the existence of a monomeric form. To the best of our knowledge, another example of tin-hydroxide stabilized by a phen ligand was previously reported by Aghabozorg *et al.*, characterized by X-ray crystallographic structure as being [Sn(pydc)(phen)(OH)<sub>2</sub>]<sub>2</sub>·3H<sub>2</sub>O (pydc = pyridine-2,6-dicarboxate) [34]. The two terminal OH groups occupy the apical positions of a pentagonal bipyramid. The IR spectrum recorded from the crystals of **7** corroborates the presence of H<sub>2</sub>O and OH ligands by showing two shoulders centered at 3407 and 3213 cm<sup>−1</sup> and a sharp band at 1628 cm<sup>−1</sup> assigned to δ(H<sub>2</sub>O) elongation. The characteristic absorption bands of CF<sub>3</sub>SO<sub>3</sub> and phen are also well visible (Figure 1d). Globally, the IR fingerprint of **7** shows strong similarities to that of **5**.

Compound **7** can be viewed as a reaction intermediate resulting from the reactivity of **1** toward 1,10-phenanthroline under sub-stoichiometric phen conditions (Equation (1)). This can then lead to the formation of **5** by dimerization, driven by the nucleophilicity of the OH group, resulting in the expulsion of aqua ligands (Scheme 4). This mechanism is similar to that proposed earlier by Chandrasekhar *et al.* for the dimerization of {[*n*-Bu<sub>2</sub>Sn(OH<sub>2</sub>)<sub>4</sub>]<sup>2+</sup>[2,5-Me<sub>2</sub>C<sub>6</sub>H<sub>3</sub>SO<sub>3</sub><sup>−</sup>]<sub>2</sub> into {[*n*-Bu<sub>2</sub>Sn(μ-OH)(O<sub>3</sub>SC<sub>6</sub>H<sub>3</sub>-2,5-Me<sub>2</sub>)]<sub>2</sub>]<sub>*n*</sub> [35].



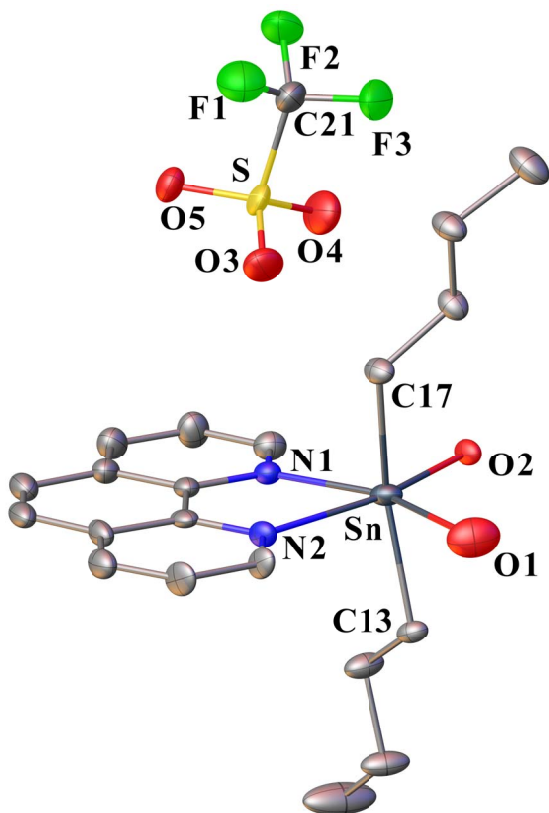


**Figure 7.** ORTEP drawing of **7** using the atom labeling scheme (30% probability thermal ellipsoids). The hydrogen atoms of O1 and O2 could not be precisely located. Selected bond lengths (Å) and angles (°): Sn–N1 2.208(11), Sn–N2 2.342(8), Sn–O1 2.512(8), Sn–O2 2.142(5), Sn–C13 2.136(17), Sn–C17 2.123(7), S–O3 1.466(7), S–O4 1.403(8), S–O5 1.408(6), C21–F1 1.311(13), C21–F2 1.309(12), C21–F3 1.330(11), C21–S 1.794(11); O1–Sn–O2 113.8(3), O2–Sn–O1 89.1(3), O2–Sn–N2 162.2(3), N1–Sn–O1 157.1(3), N1–Sn–N2 73.1(4), N2–Sn–O1 84.1(3), C13–Sn–C17 161.9(3), C13–Sn–O1 79.9(3), C13–Sn–O2 91.9(2), C13–Sn–N1 100.1(4), C13–Sn–N2 90.7(3), C17–Sn–O1 82.2(3), C17–Sn–O2 97.4(2), C17–Sn–N1 95.6(4), C17–Sn–N2 85.2(3), O3–S–C21 103.7(5), O4–S–C21 104.5(5), O4–S–O3 113.9(5), O4–S–O5 117.0(5), O5–S–C21 104.2(4), O5–S–O3 111.7(4). F1–C21–F3 109.1(11), F1–C21–S 110.5(7), F2–C21–F1 106.5(9), F2–C21–F3 106.6(9), F2–C21–S 113.1(9), F3–C21–S 110.8(7).

From a structural point of view, **7** can be related to the salt  $\{[n\text{-Bu}_2\text{Sn}(\text{OH}_2)(\text{phen})(\text{O}_3\text{SC}_6\text{H}_3\text{-}2,5\text{-Me}_2)]^+ + [2,5\text{-Me}_2\text{C}_6\text{H}_3\text{SO}_3]^- \}$  also described by Chandrasekhar *et al.*, and isolated by reacting  $\{[n\text{-Bu}_2\text{Sn}(\text{OH}_2)_4]^{2+} + [2,5\text{-Me}_2\text{C}_6\text{H}_3\text{SO}_3]^- \}_2$  with 1,10-phen [35]. The two compounds exhibit strong similarities. They consist of mononuclear hydrated diorganotin cations chelated by a phen ligand. In the Chandrasekhar cation, the coordination of the tin atom is completed by a sulfonate ligand, whereas for **7**, we claim the presence of a terminal OH group. It is interesting to note that in solution in  $\text{CD}_3\text{CN}$ , the  $^{119}\text{Sn}\{^1\text{H}\}$  NMR spectroscopic analysis of the crystals of **7** shows the presence of a mixture of four species (Figure S21), which highlights the instability of the mononuclear cation **7** also in solution. It is nevertheless possible to identify the characteristic resonances of compounds **2** (–133, –161 ppm), **4** (–139, –143 ppm), and **5** (–226 ppm). The most shielded signal at –260 ppm is thus attributed to **7**. Based on the relative integration, the two main species are **5** and **7**, which is consistent with the dimerization reaction suggested in Scheme 4. However, the presence of species **2** and **4**, which are in the minority according to a  $^{119}\text{Sn}\{^1\text{H}\}$  NMR spectrum and do not bear phen ligands, from **7**, is still unexplained.

Thus, the solid-state structure of **7** resulting from the reaction in dichloromethane differs markedly from the results obtained in acetonitrile, leading to the hypothesis of compound **3**. This implies a determining role of the solvent used on the nature of the trifluoromethanesulfonate intermediate species formed. This has already been demonstrated experimentally in the past by Otera *et al.*, who showed that when  $n\text{-Bu}_2\text{SnO}$  reacts with triflic acid in  $\text{CH}_2\text{Cl}_2$  conditions, the compound **1**, characterized as a dimeric cation is preferentially formed [8], whereas in acetonitrile, a polymeric structure prevails, alternating anhydrous and hydrated moieties of  $[n\text{-Bu}_2\text{Sn}(\text{OH})(\text{OTf})]_2$  and  $[n\text{-Bu}_2\text{Sn}(\text{OH})(\text{OTf})(\text{H}_2\text{O})]_2$ , respectively [5]. In the future, we plan to use this modularity to explore the performance of the compounds described in this study for tin-assisted organic reactions, especially since 1,10-phenanthroline derivatives are known to be efficient and stable ligands in homogeneous catalysis [36].

### 2.7. Isolation and solid-state structure of $[C_{12}H_9N_2][CF_3SO_3]$ (**phenHOTf**)

In addition to **7**, single crystals of 1,10-phenanthrolium trifluoromethanesulfonate,  $[C_{12}H_9N_2][CF_3SO_3]$  (**phenHOTf**), were obtained after a few days from the filtrate of the mother-liquor. The **phenHOTf** salt consists of a monoprotonated 1,10-phenanthrolium cation interacting with a surrounding trifluoromethanesulfonate anion through N–H···O hydrogen bonding [ $N1\cdots O3 = 2.804(2)$  Å,  $N1-H\cdots O3 = 147.61(11)^\circ$ ]. An ORTEP representation is shown in Figure 8. To date, a large number of structures of 1,10-phenanthrolium salts  $[C_{12}H_9N_2][X]$  have been resolved by X-ray crystallography, such as  $X = Cl^-$  [37],  $BPh_4^-$  [38],  $I_3^-$  [39],  $PF_6^-$  [40]. The structure of **phenHOTf** is a new example. The crystal stacking of **phenHOTf** (Figure 9) shows that the phenanthrolium cations are grouped in pairs *via* offset  $\pi$ - $\pi$  interactions characterized by an interplanar distance of 3.398 Å, a centroid-centroid distance of 4.878 Å, and a slippage distance of 3.50 Å (slippage angle = 45.85°).

### 2.8. Reactivity of **1** to 2,9-dimethyl-1,10-phenanthroline

Subsequently, the reactivity of **1** was extended to the disubstituted 1,10-phenanthrolines. Under the reaction conditions (room temperature, dichloromethane/toluene mixture), we found that 4,7-diphenyl-1,10-phenanthroline (bathophenanthroline) did not react, fully recovering the starting compounds. However, in the presence of 2,9-dimethyl-1,10-phenanthroline (**dmphen**), two types of colorless crystals were successively obtained from the mother liquor. Monitoring of the reaction by  $^{119}Sn\{^1H\}$  NMR in  $CD_2Cl_2$  revealed the transformation of **1** into distannoxanes **2** and **4**. However, we did not detect the formation of organotin species coordinated by **dmphen** ligands, as in the case of compounds **5**, **6** and **7**. This is probably due to steric hindrance caused by the presence of methyl substituents. The first type of crystals collected as long needles was characterized by X-ray diffraction analysis as being the organic salt  $[C_{14}H_{13}N_2][CF_3SO_3]$  (**dmphenHOTf**). An ORTEP representation is shown in Figure 10. The monoprotonation of **dmphen** led to the formation of the cation  $[C_{14}H_{13}N_2]^+$ . The

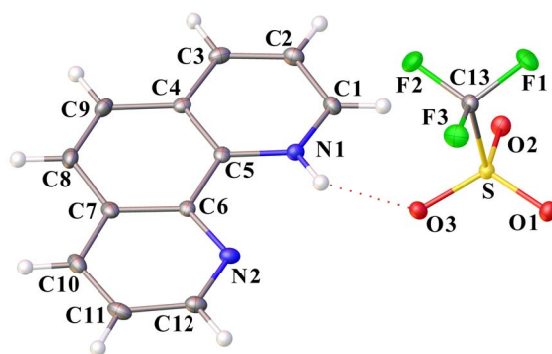


**Figure 8.** ORTEP drawing of **phenHOTf** using the atom labeling scheme (30% probability thermal ellipsoids). The N–H···O interaction is indicated by a red dotted line. Selected bond lengths (Å) and angles ( $^\circ$ ): C1–N1 1.333(2), C5–N1 1.358(2), C5–C6 1.438(3), C6–N2 1.359(2), C12–N2 1.326(3), O1–S 1.4367(14), O2–S 1.4417(14), O3–S 1.4505(14), C13–S 1.825(2), C13–F1 1.336(2), C13–F2 1.335(2), C13–F3 1.335(2); C1–N1–C5 123.04(17), C12–N2–C6 116.54(18), O1–S–C13 103.50(9), O1–S–O2 115.68(8), O1–S–O3 114.80(8), O2–S–C13 103.31(9), O2–S–O3 114.88(8), O3–S–C13 102.07(9), F1–C13–F3 107.57(16), F1–C13–S 111.34(13), F2–C13–F1 107.49(16), F2–C13–F3 107.62(15), F2–C13–S 111.31(14), F3–C13–S 111.31(14).

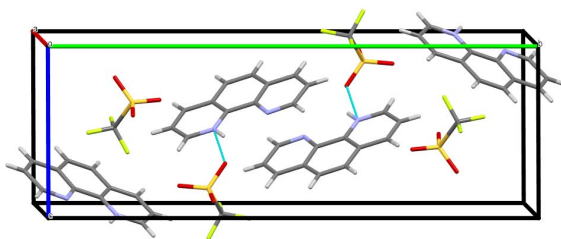


**Figure 9.** Crystal packing of **phenHOTf** along the *a*-axis. (MERCURY representation [27], color code: N = blue, C = gray, H = white, O = red, S = yellow, F = green.)

positive charge is balanced by a triflate anion, which is also involved in hydrogen bonding to the cation *via* an N–H···O interaction [ $N1\cdots O1 = 2.910$  Å,  $N1-H1\cdots O1 = 157.63(14)^\circ$ ]. The crystal packing view of **dmphenHOTf** shows a folded sheet organization

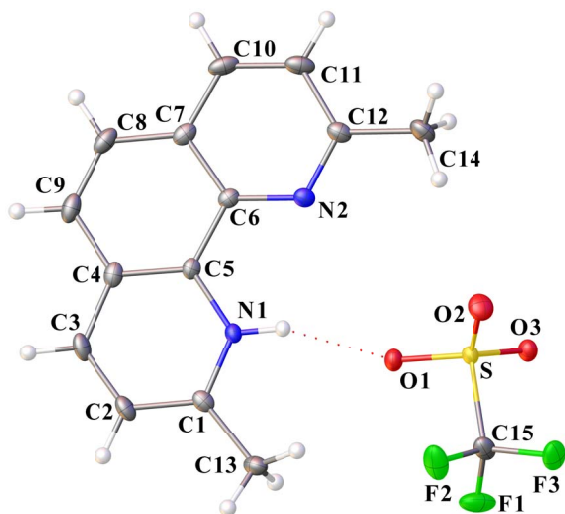


**Figure 10.** ORTEP drawing of **dmphenHOTf** using the atom labeling scheme (30% probability thermal ellipsoids). The N–H···O interaction is indicated by a red dotted line. Selected bond lengths (Å) and angles (°): N1–C5 1.371(3), N1–C1 1.336(3), N2–C6 1.355(3), N2–C12 1.327(3), S–O1 1.4472(17), S–O2 1.4306(19), S–O3 1.4359(17), S–C15 1.832(3), F1–C15 1.329(3), F2–C15 1.334(3), F3–C15 1.336(3); O1–S–C15 102.31(11), O3–S–O1 115.26(11), O3–S–C15 103.14(12), O2–S–O1 115.68(12), O2–S–O3 114.96(11), O2–S–C15 102.71(14), F2–C15–S 111.2(2), F2–C15–F3 107.5(2), F3–C15–S 111.46(18), F1–C15–S 111.25(18), F1–C15–F2 108.1(2), F1–C15–F3 107.2(2).

(Figure 11), stacked along the *a*-axis via  $\pi$ – $\pi$  interactions between the aryl rings of  $[\text{C}_{14}\text{H}_{13}\text{N}_2]^+$  with an interplanar distance of 3.449 Å, a centroid–centroid distance of 3.626 Å, and a slippage distance of 1.119 Å (slip angle of 17.98°). Recently, *Assefa* and *Gore* unintentionally obtained the same compound by adding 2,9-dimethyl-1,10-phenanthroline drop wise to a  $\text{Eu}(\text{CF}_3\text{O}_3\text{S})_3$  solution [41]. In addition, several structures of 2,9-dimethyl-1,10-phenanthroline salts  $[\text{C}_{14}\text{H}_{13}\text{N}_2][\text{X}]$  have already been solved. This is the case for  $\text{X} = \text{ClO}_4^-$  [42],  $\text{Cl}^-$  [43],  $\text{NO}_3^-$  [44],  $\text{PF}_6^-$  [45].

A second type of colorless crystals, exhibiting a different shape (prism), was collected from the filtrate of the solution from which **dmphenHOTf** crystals were initially obtained. Their composition consists of a monoprotonated dmphen mole-

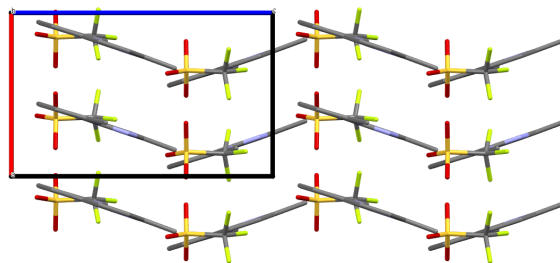


**Figure 11.** Organization of **dmphenHOTf** in the crystal lattice along the *a*-axis. Hydrogen atoms are omitted for clarity (MERCURY representation [27], color code: N = blue, C = gray, O = red, S = yellow, F = green).

cule (**dmphenH**) co-crystallizing with a free dmphen molecule to form **dmphenHOTf·dmphen**. The two components interact through an N–H···N hydrogen bond [ $\text{N1}\cdots\text{N3} = 2.927(3)$  Å]. In fact, the hydrogen atom is split between the two nitrogen atoms [ $\text{N1}\cdots\text{H}\cdots\text{N3} = 152.78(14)^\circ$ ,  $\text{N3}\cdots\text{H}\cdots\text{N1} = 159.92(14)^\circ$ ]. Interestingly, the steric hindrance of the methyl substituents leads to a positioning close to orthogonality between the two heterocycles. Their arrangement can be described as a head–tail assembly. A dihedral angle of  $77.74(3)^\circ$  was determined between the two planes containing dmphenH and dmpe. The overall positive charge is compensated by the presence of a triflate anion. An ORTEP view of **dmphenHOTf·dmphen** is shown in Figure 12. The crystal packing view, depicted in Figure 13, also shows that the dmphen rings are in  $\pi$ – $\pi$  aromatic interaction and are organized in pairs. However, two distinctive stacking patterns can be observed for **dmphen** and **dmphenH**, respectively, characterized by interplanar distances of 3.631 and 3.353 Å, centroid–centroid distances of 3.762 Å and 4.445 Å, and slip distances of 0.984 Å (slip angle of 15.16°) and 2.918 Å (slip angle of 41.03°), respectively.

In the past, we have shown the possibility of accessing phenazinium and acridinium trifluoromethanesulfonate salts by reacting compound **1**, at room temperature, in the presence of phenazine (phz) [12] and acridine (acr) [46], respectively. The isolation of original architectures based on molecular stacks driven by hydrogen and  $\pi$ – $\pi$  interactions, has underlined the predisposition of *N*-heterocyclic molecules as suitable building-blocks. In our opinion, this approach, *via* the assistance of an organotin



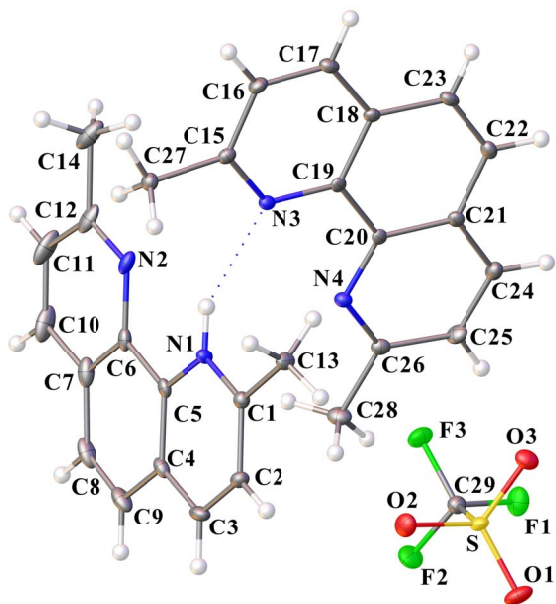


**Figure 12.** ORTEP drawing of **dmphenHOTf-dmphen** using the atom labeling scheme (30% probability thermal ellipsoids). The N–H···N interaction is indicated by a blue dotted line. Selected bond lengths (Å) and angles (°): C1–N1 1.336(3), C5–N1 1.366(3), C6–N2 1.366(3), C12–N2 1.324(3), C15–N3 1.335(3), C19–N3 1.367(3), C20–N4 1.357(3), C26–N4 1.330(3), C29–F1 1.334(3), C29–F2 1.333(3), C29–F3 1.340(3), C29–S 1.832(3), O1–S 1.4364(18), O2–S 1.4423(19), O3–S 1.4426(18); F2–C29–F3 107.3(2), F2–C29–F1 107.4(2), F2–C29–S 111.80(18), F3–C29–S 110.85(17), F1–C29–F3 107.1(2), F1–C29–S 112.11(17), O2–S–C29 102.19(12), O2–S–O3 114.84(11), O3–S–C29 103.17(11), O1–S–C29 103.78(11), O1–S–O2 115.20(12), O1–S–O3 115.13(12).

compound, could be seen as an innovative method of crystal engineering. It is successfully applied here to 1,10-phenanthroline and 2,9-dimethyl-1,10-phenanthroline, leading to new phenanthroline trifluoromethanesulfonate salts.

### 3. Conclusion and perspectives

In conclusion, the study of the reactivity between 1,10-phenanthroline (phen) and the complex  $[n\text{-Bu}_2\text{Sn}(\mu\text{-OH})(\text{H}_2\text{O})(\text{CF}_3\text{SO}_3)_2]$  (**1**) led to the com-

plete characterization of two new di-*n*-butyltin(IV) trifluoromethanesulfonates, **5** and **6**, *N,N*-bis-chelated with phen ligands. Furthermore, using  $^{119}\text{Sn}(^1\text{H})$  NMR spectroscopy as an investigation probe under deuterated acetonitrile conditions, we were also able to highlight the formation of additional tin trifluoromethanesulfonate intermediates. Two, **2** and **4**, exhibiting distannoxane-like frameworks but without phen-coordinated ligands, were clearly identified by comparison with previous work while investigations were conducted to clarify the unknown  $^{119}\text{Sn}(^1\text{H})$  NMR fingerprint attributed to **3**. Crystallization attempts are underway to corroborate the suggested dinuclear structure. We also observed that the identity of the solvent used for the reaction had a notable impact on the intermediates formed. In the presence of dichloromethane, the solid-state structure of a mononuclear hydrated di-*n*-butyltin hydroxide, stabilized by a phen ligand and assigned to **7**, was revealed. To the best of our knowledge, there are few comparable examples to date. Thus, new structural and spectroscopic insights into organotin(IV) trifluoromethanesulfonates have been obtained, thereby opening the way for further investigations. In the future, we plan to explore the catalytic properties of these compounds.

## 4. Experimental section

### 4.1. Materials and instrumentation

Organic solvents, dichloromethane (Carlo Erba, 99.5% purity), toluene (Acros, 99.99%), acetonitrile (99.9% purity), were refluxed over appropriate dessicants, distilled, and saturated with argon prior to use. Chemicals were purchased from Aldrich, Acros Organics, and Fluka and used without further purification. The starting compound  $[n\text{-Bu}_2\text{Sn}(\text{OH})(\text{H}_2\text{O})(\text{CF}_3\text{SO}_3)_2]$  (**1**) was synthesized from *n*-Bu<sub>2</sub>SnO (Acros, 98% purity) and trifluoromethanesulfonic acid (Fluka, 98% purity) in acetonitrile, according to a published method [8]. The  $^1\text{H}$ ,  $^{19}\text{F}$ ,  $^{119}\text{Sn}\{^1\text{H}\}$ , and  $^{13}\text{C}\{^1\text{H}\}$  NMR experiments were recorded on Bruker Avance 300 and 500 MHz spectrometers and calibrated with Me<sub>4</sub>Si, trifluoromethylbenzene, or Me<sub>4</sub>Sn as an internal standard. Chemical shift  $\delta$  values are given in ppm. FT-IR spectra were recorded on a Bruker Alfa spectrometer equipped with a Specac Golden Gate™ ATR device.



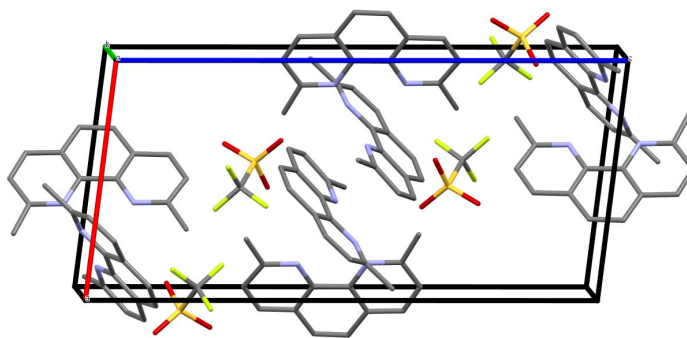


**Figure 13.** Crystal packing of **dmphenHOTf·dmphen** along the *b*-axis. Hydrogen atoms are omitted for clarity (MERCURY representation [27], color code: N = blue, C = gray, O = red, S = yellow, F = green).

ESI-MS spectra were obtained on a Bruker micro Q-TOF instrument using acetonitrile, dichloromethane and methanol mobile phases. Elemental analyses (C, H, N, S) were performed at the Institut de Chimie Moléculaire de l'Université de Bourgogne, Dijon.

#### 4.2. Preparation of $[n\text{-Bu}_2\text{Sn}(\text{OH})(\text{phen})_2][\text{CF}_3\text{SO}_3]_2$ (**5**) and $[n\text{-Bu}_2\text{Sn}(\text{Phen})_2][\text{CF}_3\text{SO}_3]$ (**6**) from $[n\text{-Bu}_2\text{Sn}(\text{OH})(\text{H}_2\text{O})(\text{CF}_3\text{SO}_3)]_2$ (**1**) and 1,10-phenanthroline

Two molar equivalents of 1,10-phenanthroline ( $\text{C}_8\text{H}_8\text{N}_2$ , Sigma-Aldrich, 99% purity) (0.130 g, 0.72 mmol) were added to a colourless solution of  $[n\text{-Bu}_2\text{Sn}(\text{OH})(\text{H}_2\text{O})(\text{CF}_3\text{SO}_3)]_2$  (**1**) (0.300 g, 0.360 mmol) in a mixture of dichloromethane/toluene (15 mL/10 mL). The reaction medium is stirred for 3 h at room temperature leading to a clear pinkish solution. A precipitate (0.160 g) was collected after one week of evaporation at room temperature. This corresponds to the formation of compound **6**, which was then recrystallized as fine needles in dichloromethane/toluene. Compound **5** was obtained a few days later from the reaction filtrate as colorless, parallelepipedal crystals (0.050 g). The use of four equivalents of 1,10-phenanthroline gave exclusive access to compound **6**.

**5**:  $^1\text{H}$  NMR (300 MHz,  $\text{CD}_2\text{Cl}_2$ , 301 K):  $\delta$  0.5–2.1 (m, 36H, Ant), 3.78 (br, 2H), 8.02 (m, 4H), 8.11 (s, 4H), 8.66 (m, 4H), 9.37 (m, 4H);  $^{13}\text{C}\{^1\text{H}\}$  NMR (75 MHz,  $\text{CD}_2\text{Cl}_2$ , 300 K):  $\delta$  13.4, 26.5, 27.6, 120.8 (q,  $^1J_{\text{CF}} = 320$  Hz), 125.7, 127.8, 130.1, 139.9, 141.7, 149.9;  $^{19}\text{F}$  NMR (282 MHz,  $\text{CD}_2\text{Cl}_2$ , 301 K):  $\delta$  -78.5 (s,  $\text{CF}_3\text{SO}_3^-$ );  $^{119}\text{Sn}\{^1\text{H}\}$  (186 MHz,  $\text{CD}_3\text{CN}$ , 298 K):

$\delta$  -226;  $^{119}\text{Sn}\{^1\text{H}\}$  (186 MHz, acetone- $d_6$ , 298 K):  $\delta$  -150; ESI-HRMS (+):  $m/z$  431.1133 Da (100%)  $[\text{M}-\text{OH}-\text{phen}-n\text{-Bu}_2\text{Sn}]^+$  ( $\text{C}_{20}\text{H}_{27}\text{N}_2\text{OSn}$ , calc.: 431.1145 Da); FT-IR (ATR,  $\text{cm}^{-1}$ ): 3321, 3081, 3066, 2956, 2929, 2871, 1626, 1575, 1589, 1543, 1518, 1427, 1379, 1282, 1237, 1223, 1155, 1027, 854, 731, 717, 683, 633, 573, 515. Anal. Calc. For  $\text{C}_{42}\text{H}_{54}\text{F}_6\text{N}_4\text{O}_8\text{S}_2\text{Sn}_2$  (1158.44): C, 43.55; H, 4.70; N, 4.84; S, 5.54. Found: C, 43.42; H, 5.45; N, 4.90; S, 4.32%.

**6**:  $^1\text{H}$  NMR (500 MHz, acetone- $d_6$ , 298 K): 0.65 (t,  $J = 7.3$  Hz, 6H), 1.20 (m, 4H), 1.34 (m, 4H), 2.10 (m, 4H), 8.26 (m, 4H), 8.50 (s, 4H), 9.18 (m, 8H);  $^{13}\text{C}\{^1\text{H}\}$  NMR (125 MHz, acetone- $d_6$ , 298 K):  $\delta$  13.1, 26.5, 27.8, 27.81, 121.9 (q,  $^1J_{\text{CF}} = 321$  Hz), 127.20, 128.7, 131.0, 138.5, 142.9, 149.0;  $^{19}\text{F}$  NMR (470 MHz, acetone- $d_6$ , 298 K):  $\delta$  -78.8 (s,  $\text{CF}_3\text{SO}_3^-$ );  $^{119}\text{Sn}\{^1\text{H}\}$  (186 MHz, acetone- $d_6$ , 298 K):  $\delta$  -231; ESI-HRMS (+):  $m/z$  445.1305 Da (100%)  $[\text{M}-\text{phen}+\text{OCH}_3]^+$  ( $\text{C}_{21}\text{H}_{29}\text{N}_2\text{OSn}$ , calc.: 445.1301 Da),  $m/z$  431.11559 Da (80%)  $[\text{M}-\text{phen}+\text{OH}]^+$  ( $\text{C}_{20}\text{H}_{27}\text{N}_2\text{OSn}$ , calc.: 431.11454 Da); FT-IR (ATR,  $\text{cm}^{-1}$ ): 3104, 3070, 2960, 2925, 2870, 2860, 1630, 1589, 1543, 1523, 1431, 1259, 1223, 1153, 1027, 868, 720, 633, 573, 516. Anal. Calc. For  $\text{C}_{34}\text{H}_{34}\text{F}_6\text{N}_4\text{O}_6\text{S}_2\text{Sn}$  (891.49): C, 45.81; H, 3.84; N, 6.28; S, 7.19 Found: C, 45.56; H, 3.38; N, 6.30; S, 7.29%.

#### 4.3. Isolation and characterization of **3**

The protocol used the same conditions as those used in the  $^{119}\text{Sn}\{^1\text{H}\}$  NMR experiment shown in Figure 5d. One molar equivalent of 1,10-phenanthroline (0.065 g, 0.360 mmol) was added to a colourless solution of  $[n\text{-Bu}_2\text{Sn}(\text{OH})(\text{H}_2\text{O})(\text{CF}_3\text{SO}_3)]_2$  (**1**) (0.300 g, 0.360 mmol) in a mixture of acetonitrile/toluene

(15 mL/10 mL). The solution was progressively enriched in compound **3** by eliminating species **2**, **3**, and **4** by successive crystallizations, and the filtrate was stored each time at  $-20^{\circ}\text{C}$ . **3** was finally obtained after three cycles ( $^{119}\text{Sn}\{^1\text{H}\}$  NMR monitoring) and after the total evaporation of the solvents leading to a colorless pasty solid.

**3**:  $^1\text{H}$  NMR (499 MHz,  $\text{CD}_3\text{CN}$ , 298 K): 0.61 (t,  $J = 7.0$  Hz, 6H), 1.09 (m, 4H), 1.17 (m, 4H), 2.08 (m, 4H), 8.36 (m, 2H), 8.41 (s, 2H), 9.13 (m, 2H), 9.53 (m, 2H);  $^{13}\text{C}\{^1\text{H}\}$  NMR (125 MHz,  $\text{CD}_3\text{Cl}_2$ , 298 K): 13.1, 25.9, 27.3, 33.9, 120.55 ( $^1J_{\text{CF}} = 319$  Hz), 127.2, 128.6, 130.9, 139.4, 143.0, 150.3;  $^{19}\text{F}$  NMR (470 MHz,  $\text{CH}_2\text{Cl}_2$ , 298 K):  $\delta -78.4$  (s,  $\text{CFSO}_3$ );  $^{119}\text{Sn}\{^1\text{H}\}$  (149 MHz,  $\text{CD}_3\text{CN}$ , 298 K):  $\delta -266$ ,  $^{119}\text{Sn}\{^1\text{H}\}$  (186 MHz,  $\text{CD}_2\text{Cl}_2$ , 298 K):  $\delta -288$ ; ESI MS (+):  $m/z$  1275.07507 Da (100%)  $[\text{M}]^+$  ( $\text{C}_{43}\text{H}_{52}\text{O}_9\text{N}_4\text{F}_9\text{S}_3\text{Sn}_2$ , calc.: 1275.07912 Da),  $m/z$  893.0887 Da (67%)  $[\text{M}+\text{H}-\text{phen}-n\text{-Bu}_2\text{Sn}]^+$  ( $\text{C}_{34}\text{H}_{35}\text{O}_6\text{N}_4\text{F}_6\text{S}_2\text{Sn}$ , calc.: 893.09201 Da),  $m/z$  563.06134 Da ( $z = 1$ , 67%)  $[n\text{-Bu}_2\text{Sn}(\text{phen})(\text{CF}_3\text{SO}_3)]^+$  ( $\text{C}_{21}\text{H}_{26}\text{O}_3\text{N}_2\text{F}_3\text{SSn}$ , calc.: 563.06328 Da); FT-IR (ATR,  $\text{cm}^{-1}$ ): 3091, 3071, 2960, 2931, 2871, 1631, 1607, 1586, 1525, 1264, 1200, 1162, 1016, 866, 723, 691, 631, 573, 513, 426. Anal. Calc. For  $\text{C}_{44}\text{H}_{52}\text{F}_{12}\text{N}_4\text{O}_{12}\text{S}_4\text{Sn}_2$  (1422.57): C, 37.15; H, 3.68; N, 3.94; S, 9.02 Found: C, 36.43; H, 3.74; N, 4.13; S, 8.16%.

#### 4.4. Isolation and characterization of *phenHOTf*

Small crystals of **phenHOTf** were obtained from the filtrate of the mother-liquor from which compound **7** had been isolated.

**phenHOTf**:  $^1\text{H}$  NMR (500 MHz,  $\text{CD}_2\text{Cl}_2$ , 298 K):  $\delta 8.03$  (dd, 1H,  $J = 8.17, 5.02$  Hz), 8.08 (s, 1H), 8.16 (brs, 2H), 8.71 (d, 1H,  $J = 8.12$  Hz), 8.79 (d, 1H,  $J = 7.30$  Hz), 9.36 (d, 1H,  $J = 4.35$  Hz), 9.64 (brs, 1H);  $^{19}\text{F}$  NMR (470 MHz,  $\text{CD}_2\text{Cl}_2$ , 298 K):  $\delta -78.57$  (s,  $\text{CFSO}_3$ );  $^{13}\text{C}\{^1\text{H}\}$  NMR (125 MHz,  $\text{CD}_2\text{Cl}_2$ , 298 K): 120.4 ( $^1J_{\text{CF}} = 320$  Hz), 125.6, 126.6, 127.5, 129.8, 130.3, 137.8, 141.4, 147.8, 150.5; FT-IR (ATR,  $\text{cm}^{-1}$ ): 3100, 3070, 3043, 2960, 2930, 2872, 1598, 1542, 1525, 1497, 1471, 1438, 1283, 1223, 1152, 10256, 847, 719, 632, 571, 514, 463.

#### 4.5. Isolation and characterization of *dmphenHOTf* and *dmphenHOTf·dmphen*

Four molar equivalents of 2,9-dimethyl-1,10-phenanthroline ( $\text{C}_{10}\text{H}_{12}\text{N}_2$ , Sigma-Aldrich, 99%

purity) (0.200 g, 0.96 mmol) were added to a colourless solution of  $[n\text{-Bu}_2\text{Sn}(\text{OH})(\text{H}_2\text{O})(\text{CF}_3\text{SO}_3)]_2$  (**1**) (0.200 g, 0.24 mmol) in a dichloromethane/toluene mixture (10 mL/5 mL). The reaction medium is stirred for 3 h at room temperature in ambient air. In the following days, **dmphenHOTf** crystals first grew and then, after filtration of the mother-liquor, new crystals characterized as **dmphenHOTf·dmphen** were collected.

**dmphenHOTf**:  $^1\text{H}$  NMR (300 MHz,  $\text{CD}_2\text{Cl}_2$ , 299 K):  $\delta 8.65$  (d, 2H,  $J = 8.4$  Hz), 8.08 (s, 2H), 7.90 (d, 2H,  $J = 8.4$  Hz), 7.66 (br, 1H), 3.18 (s, 6H,  $\text{CH}_3$ );  $^{19}\text{F}$  NMR (470 MHz,  $\text{CD}_2\text{Cl}_2$ , 298 K):  $\delta -78.93$  (s,  $\text{CFSO}_3$ );  $^{13}\text{C}\{^1\text{H}\}$  NMR (125 MHz,  $\text{CD}_2\text{Cl}_2$ , 298 K): 23.3, 121.2 ( $^1J_{\text{CF}} = 320$  Hz), 126.8, 126.9, 128.2, 137.4, 141.5, 159.9; FT-IR (ATR,  $\text{cm}^{-1}$ ): 3174, 3111, 3046, 3016, 2980, 1635, 1604, 1533, 1503, 1463, 1278, 1253, 1246, 1222, 1142, 1032, 813, 719, 691, 677, 631, 573, 542, 513; Anal. Calc. For  $\text{C}_{15}\text{H}_{13}\text{F}_3\text{N}_2\text{O}_3\text{S}$  (358.34): C, 50.28; H, 3.66; N, 7.829; S, 8.95. Found: C, 49.96; H, 4.05; N, 7.82; S, 6.29%.

**dmphenHOTf·dmphen**:  $^1\text{H}$  NMR (500 MHz,  $\text{CD}_2\text{Cl}_2$ , 298 K):  $\delta 8.33$  (d, 4H,  $J = 8.30$  Hz), 7.84 (s, 4H), 7.57 (d, 4H,  $J = 8.38$  Hz), 7.41 (br, 1H), 2.59 (s, 12H,  $\text{CH}_3$ );  $^{19}\text{F}$  NMR (470 MHz,  $\text{CD}_2\text{Cl}_2$ , 298 K):  $\delta -78.92$  (s,  $\text{CFSO}_3$ );  $^{13}\text{C}\{^1\text{H}\}$  NMR (125 MHz,  $\text{CD}_2\text{Cl}_2$ , 298 K): 23.6, 121.3 ( $^1J_{\text{CF}} = 321$  Hz), 125.4, 126.4, 127.96, 139.08, 141.7, 159.1; FT-IR (ATR,  $\text{cm}^{-1}$ ): 2958, 2929, 2858, 1636, 1626, 1605, 1595, 1541, 1499, 1466, 1353, 1257, 1221, 1152, 1027, 853, 754, 735, 724, 634, 570, 546, 515, 441; Anal. Calc. For  $\text{C}_{29}\text{H}_{25}\text{F}_3\text{N}_4\text{O}_3\text{S}$  (566.59): C, 61.47; H, 4.45; N, 9.89; S, 5.66. Found: C, 60.93; H, 4.80; N, 10.08; S, 5.09%.

#### 4.6. X-ray diffraction analysis and refinement

Crystallographic data and structure refinement details for **5**, **6**, **7**, **phenHOTf**, **dmphenHOTf** and **dmphenHOTf·dmphen** are reported and detailed in *Supporting information – Crystallographic Data*.

#### Declaration of interests

The authors do not work for, advise, own shares in, or receive funds from any organization that could benefit from this article, and have declared no affiliations other than their research organizations.

## Funding

The authors are grateful to the University of Burgundy-Dijon and the CNRS for their constant financial support.

## Acknowledgements

The authors would particularly like to thank Dr. Q. Bonin, Ms M.-J. Penouilh (ESI-HRMS) and Ms T. Régnier (elemental analysis), as well as the Professor Klaus Jurkschat and the second anonymous reviewer for their corrections and suggestions, which significantly improved the initial manuscript.

## Supplementary data

Supporting information for this article is available on the journal's website under <https://doi.org/10.5802/crchim.260> or from the author.

Additional spectroscopic data ( $^1\text{H}$ ,  $^{19}\text{F}$ ,  $^{13}\text{C}\{^1\text{H}\}$ ,  $^{119}\text{Sn}\{^1\text{H}\}$ , FT-IR, and ESI-MS spectra; Figures S1–S21) related to complexes **5**, **6**, **7** are given in *Supporting Information—Spectroscopic Data*. Crystallographic data regarding the X-ray structures reported in this study (compounds **5**, **6**, **7**, **phenHOTf**, **dmphenHOTf**, and **dmphenHOTf-dmphen**) are available in *Supporting Information—Crystallographic Data*.

CCDC 2254272 (**5**), 2254273 (**6**), 2254274 (**7**), 2254275 (**phenHOTf**), 2254276 (**dmphenHOTf**), and 2254277 (**dmphenHOTf-dmphen**) contain the supplementary crystallographic data for this paper. These data can be obtained free of charge from the Cambridge Crystallographic Data Centre via [www.ccdc.cam.ac.uk/data\\_request/cif](http://www.ccdc.cam.ac.uk/data_request/cif).

## References

- [1] M. Schmeisser, P. Sartori, B. Lippsmeier, *Chem. Ber.*, 1970, **103**, 868–879.
- [2] T. Sato, Y. Wakahara, J. Otera, H. Nozaki, *Tetrahedron*, 1991, **47**, 9773–9782.
- [3] T. Sato, Y. Wakahara, J. Otera, H. Nozaki, *Tetrahedron Lett.*, 1990, **31**, 1581–1584.
- [4] K. Sakamoto, Y. Hamada, H. Akashi, A. Orita, J. Otera, *Organometallics*, 1999, **18**, 3555–3557.
- [5] H. Lee, J. Y. Bae, O. S. Kwon, S. J. Kim, S. D. Lee, H. S. Kim, *J. Organomet. Chem.*, 2004, **689**, 1816–1820.
- [6] J.-C. Choi, K. Kohno, Y. Ohshima, H. Yasuda, T. Sakakura, *Catal. Commun.*, 2008, **9**, 1630–1633.
- [7] P. Švec, R. Olejník, Z. Padělková, A. Růžička, L. Plasseraud, *J. Organomet. Chem.*, 2012, **708–709**, 82–87.
- [8] K. Sakamoto, H. Ikeda, H. Akashi, T. Fukuyama, A. Orita, J. Otera, *Organometallics*, 2000, **19**, 3242–3248.
- [9] A. Orita, J. Xiang, K. Sakamoto, J. Otera, *J. Organomet. Chem.*, 2001, **624**, 287–293.
- [10] D. Ballivet-Tkatchenko, H. Cattey, L. Plasseraud, P. Richard, *Acta Crystallogr.*, 2006, **E62**, m2820–m2822.
- [11] P. B. Hitchcock, M. F. Lappert, G. A. Lawless, G. M. de Lima, L. J.-M. Pierssens, *J. Organomet. Chem.*, 2000, **601**, 142–146.
- [12] L. Plasseraud, H. Cattey, P. Richard, D. Ballivet-Tkatchenko, *J. Organomet. Chem.*, 2009, **694**, 2386–2394.
- [13] J. Beckmann, *Appl. Organomet. Chem.*, 2005, **19**, 494–499.
- [14] L. Plasseraud, H. Cattey, P. Richard, *Z. Naturforsch.*, 2010, **65b**, 1293–1300.
- [15] L. Plasseraud, H. Cattey, P. Richard, *Z. Naturforsch.*, 2011, **66b**, 262–268.
- [16] A. Orita, K. Sakamoto, H. Ikeda, J. Xiang, J. Otera, *Chem. Lett.*, 2001, **30**, 40–41.
- [17] A. Orita, J. Xiang, K. Sakamoto, J. Otera, *J. Organomet. Chem.*, 2001, **624**, 287–293.
- [18] L. Plasseraud, B. Therrien, A. Růžička, H. Cattey, *Inorg. Chim. Acta*, 2012, **380**, 50–56.
- [19] G. A. Lawrance, *Chem. Rev.*, 1986, **86**, 17–33.
- [20] D. H. Johnston, D. F. Shriver, *Inorg. Chem.*, 1993, **32**, 1045–1047.
- [21] S. J. Angus-Dunne, L. E. P. Lee Chin, R. C. Burns, G. A. Lawrance, *Transit. Met. Chem.*, 2006, **31**, 268–275.
- [22] E. König, K. Madeja, *Spectrochim. Acta*, 1964, **43**, 45–54.
- [23] F. E. Jian, H. L. Xiao, H. X. Wang, K. Jiao, *J. Korean Chem. Soc.*, 2003, **47**, 26–30.
- [24] D. Ballivet-Tkatchenko, H. Chermette, L. Plasseraud, O. Walter, *Dalton Trans.*, 2006, 5167–5175.
- [25] I. Lange, O. Moers, A. Blaschette, P. G. Jones, *Z. Anorg. Allg. Chem.*, 1997, **623**, 1665–1671.
- [26] A. Wirth, O. Moers, A. Blaschette, P. G. Jones, *Z. Anorg. Allg. Chem.*, 2000, **626**, 529–535.
- [27] C. F. Macrae, I. J. Bruno, J. A. Chisholm, P. R. Edgington, P. McCabe, E. Pidcock, L. Rodriguez-Monge, R. Taylor, J. Van de Streek, P. A. Wood, *Appl. Crystallogr.*, 2008, **41**, 466–470.
- [28] C. Janiak, *J. Chem. Soc. Dalton Trans.*, 2000, 3885–3896.
- [29] R. Shankar, P. Chauhan, E. Jakhar, A. Dubey, G. Kociok-Köhn, *Inorg. Chem.*, 2023, **62**, 2181–2187.
- [30] A. G. Davis, *Organotin Chemistry*, Wiley-VCH, Weinheim, 2004, 179 pages.
- [31] H. Reuter, H. Puff, *J. Organomet. Chem.*, 1989, **379**, 223–234.
- [32] H. K. Sharma, F. Cervantes-Lee, J. S. Mahmoud, K. H. Pannell, *Organometallics*, 1999, **18**, 399–403.
- [33] A. Růžička, Z. Padělková, P. Švec, V. Pejchal, L. Česlová, J. Holeček, *J. Organomet. Chem.*, 2013, **732**, 47–57.
- [34] H. Aghabozorg, F. Ramezanipour, B. Nakhjavan, J. Soleimannejad, J. Attar Gharamaleki, M. A. Sharif, *Cryst. Res. Technol.*, 2007, **42**, 1137–1144.
- [35] V. Chandrasekhar, P. Singh, K. Gopal, *Organometallics*, 2007, **26**, 2833–2839.
- [36] K. Hensen, B. Spangenberg, M. Bolteb, *Acta Crystallogr.*, 2000, **C56**, 208–210.
- [37] M.-Y. Hu, Q. He, S.-J. Fan, Z.-C. Wang, L.-Y. Liu, Y.-J. Mu, Q. Peng, S.-F. Zhu, *Nature Commun.*, 2018, **9**, article no. 221.

- [38] P. K. Bakshi, T. S. Cameron, O. Knop, *Can. J. Chem.*, 1996, **74**, 201-220.
- [39] M. Bujak, W. Frank, *Z. Kristallogr. New Cryst. Struct.*, 2014, **229**, 379-380.
- [40] B. Milani, A. Anzilutti, L. Vicentini, A. Sessanta, O. Santi, E. Zangrando, S. Geremia, G. Mestroni, *Organometallics*, 1997, **16**, 5064-5075.
- [41] Z. Assefa, S. B. Gore, *Bull. Chem. Soc. Ethiop.*, 2016, **30**, 231-239.
- [42] A. Morsali, *Anal. Sci.: X-Ray Struct. Anal.*, 2005, **21**, x21-x22 (Online).
- [43] D. E. Braun, K. Raabe, A. Schneeberger, V. Kahlenberg, U. J. Griesser, *Molecules*, 2017, **22**, article no. 2238.
- [44] Y.-Q. Yu, C.-F. Ding, M.-L. Zhang, X.-M. Li, S.-S. Zhang, *Acta Crystallogr.*, 2006, **E62**, o2187-o2189.
- [45] J. H. Buttery, P. C. J. Effendy, S. Mutrofin, B. W. Skelton, C. R. Whitaker, A. H. White, *Z. Anorg. Allg. Chem.*, 2006, **632**, 1326-1339.
- [46] L. Plasseraud, H. Cattey, *C. R. Chim.*, 2013, **16**, 613-620.